

**ESTIMATING THE LEAF AREA INDEX OF *EUCALYPTUS DUNNII* IN THE MIDLANDS AREA, KWAZULU-NATAL PROVINCE OVER TWO SEASONS USING VEGETATION INDICES AND IMAGE TEXTURE MEASURES DERIVED FROM WORLDVIEW-3 IMAGERY**

By

Nokukhanya Fundiswa Mthembu



Submitted in fulfilment of the academic requirements for the degree of Master of Science in  
the Discipline of Geography in the

School of Agricultural, Earth and Environmental Sciences.

College of Agriculture, Engineering and Science.

University of KwaZulu-Natal, Pietermaritzburg

February 2022

## Abstract


Leaf Area Index (LAI) remains one of the important forest structural attributes, accurate estimations of LAI are crucial as LAI is a major input variable for 3-PGS to predict growth of different commercial forest species and their water use. While remote sensing offers a faster and effective means of estimating LAI, LAI is seldom available at spatio-temporal scales that can be used to guide and inform management decisions for localised applications. Furthermore, the knowledge relating to spatial and temporal variation of LAI is still limited. This study sought to estimate LAI of *Eucalyptus dunnii* in the Midlands area using vegetation indices and texture measures derived from WorldView-3 imagery. The first objective was to review previous work on remote sensing methods of estimating LAI across different forest ecosystems, crops and grasslands. The results revealed that during the last decade, the use of remote sensing to estimate and map LAI has increased for crops and natural forests. However, with regards to commercial forests and grasslands, there is still a need for more research as the number of studies is still small. The second objective was to use a combination of vegetation indices and texture measures to estimate LAI. The relationships between LAI and vegetation indices (VI), and LAI and texture were modelled using Partial Least Squares Regression (PLS-R). In terms of LAI estimation using texture, the results showed that combining two or more texture bands leads to improved LAI estimation accuracy. Although texture measures can improve LAI estimation accuracy, very few studies focusing on estimating LAI using texture measures have been published. Vegetation indices alone achieved poor LAI estimation accuracy. The best performing model incorporated texture ratios and it achieved an estimation accuracy of  $R^2=70$ , RMSE 1.21 in 2019 and  $R^2=0.72$ , M=RMSE=1.26. Overall, this study demonstrated that texture band ratios can estimate LAI of *Eucalyptus dunnii* in the Midlands area with acceptable accuracy.


**Keywords:** LAI estimation, *Eucalyptus dunnii*, Partial Least Squares Regression, texture measures, commercial forestry.


## Preface


This study was undertaken in fulfilment of a Master's Degree and presents the original work of the author. Any work taken from other authors or organizations is duly acknowledged within the text and references section.

  
.....  
Nokukhanya Mthembu  
(Student)

  
.....  
Date

  
.....  
ttering  
(Supervisor)

  
.....  
Date

  
.....  
Heyns Kotze  
(Co-supervisor)

13 June 2022  
.....  
Date

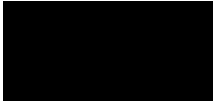
# Dedication

Dedicated to my grandmother

# Plagiarism Declaration

I, Nokukhanya Mthembu declare that;

1. The research reported in this thesis, except where otherwise indicated is my original work.
2. This thesis has not been submitted for any degree or examination at any other university.
3. This thesis does not contain other persons' data, pictures, graphs or other information, unless specifically acknowledged as being sourced from other persons.
4. This thesis does not contain other persons' writing, unless specifically acknowledged as being sourced from other researchers. Where other written sources have been quoted, then:
  - a. Their words have been re-written, and the general information attributed to them has been referenced.
  - b. Where their exact words have been used, then their writing has been placed in italics and inside quotation marks and referenced.
5. This thesis does not contain text, graphics or tables copied and pasted from the internet, unless specifically acknowledged, and the source being detailed in the thesis and reference sections.

Signed:  .....

## Acknowledgements

I would like to express my gratitude to the following individuals and institutions:

- Mondi for granting me the opportunity to further my studies and funding this project.
- University of KwaZulu-Natal, especially the School of Agricultural, Earth and Environmental Science for affording me the opportunity to pursue my Masters.
- Dr Romano Lottering, my supervisor and Heyns Kotze, my co-supervisor without you this project would not have been a possibility. Thank you for your guidance, support, advice and for pushing me to reach this point of my thesis.
- Mondi GIS department, especially my manager Miranda Wilson for supporting me.
- Mondi Growth and Yield department, especially David Borain for assisting with field data collection and processing.
- My grandmother MaKhumalo for the words of encouragement every time we spoke on the phone.
- Mr Mphande for the support and words of encouragement.
- My friends Lungile Linda, Anelisa Makhaye, Lungani Dlodla, Nosiphelo Nikani and Mandisa Makhathini for the support, encouragement and for constantly checking up on me.
- Nomthandazo Samantha Manqele and Sizwe Hlatshwayo for the support.
- Thank you Mama Siphwe Mthembu for always encouraging me to pursue my studies and for celebrating every little and big achievement in my life. May your Soul rest in peace.
- Last but not least, I want to thank myself for believing in myself, for not giving up and for doing all this hard work.

Thank you Jehovah for your Love.

# Table of Contents

Preface.....	iii
Dedication.....	iv
Table of Contents.....	vii
List of Figures.....	ix
List of Tables.....	x
List of Appendices.....	xi
1. CHAPTER ONE.....	1
1.1 Introduction.....	1
1.2 Aim.....	4
1.2.1 Objectives.....	4
1.2.2 Key research questions.....	4
1.2.3 Research structure.....	5
2. CHAPTER TWO.....	6
2.1 Introduction.....	6
2.2 Materials and Methods.....	9
2.3 Results.....	9
2.3.1 Application areas.....	10
2.3.2 Spatial distribution of LAI studies.....	11
2.3.3 Satellite data used.....	12
2.3.4 LAI estimation models used for forest, crop and grassland measures.....	14
2.3.5 Other LAI Products.....	17
2.4 Discussion.....	19
2.5 Conclusion.....	22
3. CHAPTER THREE.....	23
3.1 Introduction.....	23
3.2 Study Area.....	26
3.2.1 Introduction-general description of the study area.....	26
3.3 Data collection.....	29
3.3.1 Destructive sampling.....	29
3.3.2 Leaf area determination.....	30
3.3.3 LiCor-2200 plant canopy analyser.....	30
3.3.4 Remote sensing data acquisition and processing.....	31
3.3.5 Vegetation Indices extraction.....	32

3.3.6	Texture parameters.....	35
3.4	Statistical Analysis .....	37
3.5	Accuracy Assessment.....	37
3.6	Results .....	38
3.6.1	Descriptive Statistics.....	38
3.6.2	Optimising the PLS-R model.....	40
3.6.3	Frequency of significant variables selected by the PLS-R model .....	42
3.6.4	Mapping the spatial distribution LAI using image texture ratios and PLS-R....	44
3.6.5	Relationship between LAI and Age .....	45
4.	Discussion.....	48
4.1	The relationship between LAI and image texture ratios .....	48
4.2	Spatial distribution of LAI over the two seasons .....	49
4.3	Conclusion.....	50
5.	Synthesis.....	50
5.1	Future research and recommendations.....	51
5.2	Conclusion.....	52
5.3	Review of Objectives .....	52
5.3.1	Specific objectives reviewed.....	52
5.3.2	Concluding Remarks.....	53
References	.....	56



## List of Figures

Figure 2.1 Number of LAI studies for forest, crop and grassland .....	11
Figure 2.2 Spatial distribution and number of studies conducted at continental level .....	11
Figure 2.3 Spatial distribution and number of LAI studies conducted at country level .....	12
Figure 2.4 Sensors used to estimate LAI for forest, crop and grassland .....	13
Figure 2.5 Application of different sensor systems for forest, crop and grassland .....	14
Figure 2.6 Distribution of different model types for forest, crop and grassland LAI estimations .....	15
Figure 3.1 Map of the study area .....	29
Figure 3.2 Workflow of the methodology undertaken to meet the objectives of this study ....	29
Figure 3.3 Histogram showing LAIs over the study area in a) 2019 and b) 2022.....	39
Figure 3.4 Estimates of LAI derived from LiCor-2200 vs LAI derived from destructive sampling for a) 2019 and b) 2020 .....	40
Figure 3.5 The number of components for each model .....	41
Figure 3.6 Frequency of selected parameters: a) window size, b) WorldView-3 bands and c) Image texture parameters using the PLS-R algorithm.....	44
Figure 3.7 LAI over the study area for a) 2019 and b) 2020 using image texture ratio .....	45
Figure 3.8 Relationship between destructive sampling LAI and age .....	46
Figure 3.9 Relationship between destructive sampling LAI and age .....	47

## List of Tables

Table 2.1 Journal list and the number of articles for forest, crop and grassland .....	10
Table 3.1 General descriptions of study sites .....	27
Table 3.2 Example of destructive sampling data .....	30
Table 3.3 WorldView-3 bands .....	32
Table 3.4 Vegetation indices used in this study .....	34
Table 3.5 Texture measures used in this study .....	36
Table 3.6 Descriptive statistics for LAI values ( $m^2/ m^2$ ) measured through LiCor-2200 plant canopy analyser.....	38
Table 3.7 Descriptive statistics for direct field-based LAI, Specific LAI and Leaf Area .....	38
Table 3.8 Comparison between predictive PLS-R LAI models .....	42
Table 3.9 Top 10 selected texture ratios selected by the PLS-R algorithm in 2019 and 2020	43
Table 3.10 Showing LAI values of compartments (compt) at different phenological phases.	46

## List of Appendices

Appendix 1 Destructive sampling LAI .....	69
Appendix 2 List of countries and number of publications for each country .....	71
Appendix 3 Models and sensors used for forest, crop and grassland studies and the level of accuracy achieved by each model.....	72

## List of acronyms

°C- Degrees Celsius

3DRT- 3Dimensional Radiative Transfer

3PG - Physiological Processes Predicting Growth

ACRM-A two-layer Canopy Reflectance Model

ANN-Artificial Neural Networks

AUV-Unmanned Aerial Vehicles

ARI- Anthocyanin Reflectance Index

AVHRR-Advanced Very High Resolution Radiometer

BA-Basal Area

DAFF- Department of Agriculture, Forestry and Fisheries

DBH -Diameter at Breast Height

DEM- Digital Elevation Model

EPS-EUMETSAT Polar System

GDP - Gross Domestic Product

GDVI-Green Difference Vegetation Index

GLASS-Global Land Surface Satellite

GLCM- Grey Level Co-occurrence Matrix

GOMS-Geometric Optical Mutual Shadowing

GRNNs-General Regression Neural Networks

IEEE - Institute of Electrical and Electronics Engineers

KZN- KwaZulu-Natal

LA-Leaf Area

LAI - Leaf Area Index

LiDAR- Light detection and ranging

LUT-Look Up Tables

MISR-Multi-Angle Imaging Spectrometer

MODIS - Moderate Resolution Imaging Spectroradiometer

MSS- Multispectral Sensor

MTH-Mean Tree Height  
NDVI - Normalized Difference Vegetation Index  
NIR- Near Infrared  
PAR – Photosynthetically Active Radiation  
RMSE - Root Mean Square Error  
RTM-Radiative Transfer Model  
SI - Site Index  
SLA - Specific Leaf Area  
SMLR- Stepwise Multiple Linear Regression  
ST-Single Texture  
SR-Simple Ratio  
SVM- Support Vector Machine  
TPP - Tree per plot  
TPH - Tree per hectare  
TR-Texture Ratios  
VI -Vegetation Indices

# 1.CHAPTER ONE

## 1.1 Introduction

Commercial forests in South Africa cover approximately 1,257,341 hectares which is approximately 1% of the country's land (Kumbula et al., 2019). The most planted exotic commercial forests species are Acacia, Pinus and Eucalyptus. Eucalyptus and Acacia are generally classified as hardwood forests while Pinus is classified as softwood forest. Both soft and hardwood plantations cover approximately 39.5% surface area of KwaZulu-Natal province, with Eucalyptus being the most planted species in the Midlands area, covering approximately 30% of the planted area (DAFF, 2015). Commercial forests play a valuable role in South Africa's economy as they contribute annually towards South Africa's gross domestic product (GDP) with Eucalyptus contributing over 9% towards the total exported wood pulp, timber and non-timber products (Kumbula et al., 2019). Therefore, the development of an accurate and operational model for estimating Leaf Area Index (LAI) of *Eucalyptus* species at landscape scale is necessary, especially because LAI is a key indicator of forest health and productivity.

LAI can be defined as the total one sided area of leaf tissue per unit ground surface area (Waring, 1983). According to this definition; LAI quantitatively measures the leaf surface area available for the interception of photosynthetically active radiation (PAR) and transpiration, and is an important structural variable for describing the energy and mass exchange in a forested ecosystem (Gong et al., 1995a). LAI drives both the within and the below-canopy microclimate, controls canopy water interception, radiation extinction and carbon gas exchange, hence a key component of biogeochemical cycles in ecosystems (Potitsep et al., 2013). Any changes in canopy LAI whether caused by drought, defoliation, frost, fires or management practices are followed by changes in forest stand productivity. Process-based growth prediction models quantitatively analyse stand productivity and often LAI is the key input into such models. Additionally LAI is a significant variable incorporated into models that estimate water use and energy fluxes for commercial forests (Blinn et al., 2019).

Previously, LAI was measured through direct methods, however, there has been a shift towards using indirect methods such as vegetation indices derived from remotely sensed data. Direct techniques include destructive sampling, which is time consuming, laborious and expensive. Therefore, a faster yet effective method of predicting LAI is needed. Indirect techniques such

as remote sensing offer an opportunity to study and monitor the earth's surface at local, regional and even global scales. Furthermore; remote sensing sensors offer cost effective, high spatial and temporal resolution coverage.

One of the most common indirect methods of estimating LAI is deriving vegetation indices from remote sensing data. Several studies have demonstrated that vegetation indices can be utilised to estimate LAI accurately (Qiao et al., 2019, Li et al., 2019, Gebreslasie and van Aardt, 2011, Kross et al., 2014, Blinn et al., 2019). Mthembu (2001) studied the relationship between one of the commonly used vegetation indices known as Normalized Difference Vegetation Index (NDVI) and LAI and found that NDVI has a strong correlation with LAI and can accurately estimate the LAI of *Eucalyptus grandis x camaldulensis* with correlation coefficients of 0.78 for destructive sampling and 0.75 for the leaf canopy analyser. The results of the above mentioned study demonstrate that remote sensing offers an effective method of estimating LAI of commercial forests.

Vegetation indices (VIs) have been utilised for various remote sensing applications. They have provided accurate and reliable results in assessing vegetation health and detecting change, estimation of chlorophyll and water content in vegetation and in assessing environmental stress (Korhonen et al., 2017, Davhula, 2016). Vegetation indices often use Near Infrared (NIR) and Red regions on the electromagnetic spectrum. This is because vegetation, particularly healthy vegetation, strongly absorbs electromagnetic energy in the visible region while reflecting strongly in the NIR region, and this contrast is then used to study the status of vegetation (Blinn et al., 2019, Kross et al., 2014). However, vegetation indices do not only utilise Red and NIR portions of the electromagnetic spectrum. There are many vegetation indices that utilise other portions of the electromagnetic spectrum.

Glenn et al. (2008) concluded that remote sensing models that estimate LAI based on VIs only are subject to error and uncertainty. Therefore, additional remote sensing techniques such as texture features must be applied to improve LAI predictions. Texture features is a technique that is applied to quantify spatial variability of pixel values and patterns within an image. This technique complements spectral information with a spatial component. According to Beckschafer et al. (2013), changes in spatial distribution of vegetation can be detected through texture variation in the images and therefore texture is linked to the spatial distribution of vegetation.

Statistical techniques such as stepwise multiple linear regression (SMLR) have been used in a number of studies, however, these techniques have an inherent problem of multi-collinearity. The relationships between LAI and vegetation indices (VI) and texture with VIs were modelled using Partial Least Squares Regression (PLS-R). PLS-R is a data compression technique that is used to create predictive models from data containing highly collinear variables or factors (Chin, 1998 ; Haenlein and Kaplan, 2004; Wold, 1996).

A number of image texture techniques have been developed. For example Gebreslasie and van Aardt, (2011) identified four commonly used image texture techniques, which are model based, geometrical, statistical and signal processing. Li et al. (2019) used a combination of indices and textures to estimate LAI for rice using WV-2 image. The study demonstrated that feature texture extraction is an effective way of solving problems that are related to spectral heterogeneity and complex spatial distribution in the same category. The study used multivariate regression models to assess the potential of combining various indices and textures for the estimation of rice LAI. The study also proved that by combining textures and indices to estimate LAI, one can improve accuracy by up to twenty five percent. This study will examine a statistical image texture technique known as grey level co-occurrence matrix (GLCM) for the estimation of the LAI of *Eucalyptus dunnii* plantations. Research has shown that combining two or more texture bands leads to improved LAI estimation accuracy. Pu and Cheng (2015) used two band texture combinations to estimate forest LAI and found that texture combinations are more powerful compared to single band textures. Collecting the LAI by means of destructive sampling poses a challenge for forestry companies with large land holdings across South Africa because it is expensive, laborious, time consuming and not efficient at regional scales. The currently available LAI products are not well validated at regional levels. Therefore, there is need to develop LAI estimation techniques that are locally parameterised. This study will assess the utility of high resolution WorldView-3 vegetation indices and texture features in estimating LAI.

Models of estimating LAI are species and location specific, therefore, there is need for a model for estimating the LAI of *Eucalyptus dunnii* in the Midlands area. To the best knowledge of the researcher, no study has been conducted in South Africa to determine to what extent additional remote sensing techniques such as image texture algorithms and combined vegetation indices derived from high resolution imagery particularly WorldView-3 can improve LAI estimations for *Eucalyptus dunnii* in the Midlands area. This study investigated the following vegetation indices: Red Edge-NDVI, Green-NDVI, Simple Ratio, Modified



chlorophyll absorption ratio index 2, anthocyanin reflectance index (ARI), Red Edge triangular vegetation index (core only) and Red Edge yellow ratio. The study included Red Edge vegetation indices because Red Edge-NDVI and Green-NDVI have shown the potential to improve saturation levels compared to normal NDVI (Xie et al., 2018). Improvements in LAI estimation using remote sensing can be used to improve Physiological Processes Predicting Growth (3PGS) models.

## **1.2 Aim**

The aim of this study was to assess the ability of texture ratios computed from WorldView-3 imagery for the estimation of LAI over different seasons using PLS-R.

### *1.2.1 Objectives*

Specific objectives were to:

- Review remote sensing methods of estimating LAI for forests and crops.
- Test the utility of texture ratios in estimating LAI of *Eucalyptus dunnii* in the Midlands over two seasons using PLS-R.
- Test the utility of single texture bands in estimating LAI of *Eucalyptus dunnii* in the Midlands using PLS-R.
- Test the utility of vegetation indices in Estimating LAI of *Eucalyptus dunnii* in the Midlands over two seasons using PLS-R
- Determine the best technique in estimating LAI and map spatial distribution over the different seasons.

### *1.2.2 Key research questions*

1. What are the trends in the use of remote sensing methods to estimate LAI?
2. Are vegetation indices the best method of estimating LAI of *Eucalyptus dunnii* in the Midlands area?
3. Are texture band ratios effective in estimating LAI of *Eucalyptus dunnii* in the Midlands area?
4. Can single texture bands produce the best accuracy in estimating LAI of *Eucalyptus dunnii* in the Midlands area?
5. What is the best model in estimating LAI of *Eucalyptus dunnii* in the Midlands area using PLS-R?

### *1.2.3 Research structure*

This dissertation consists of two research papers responding to research objectives and hypotheses. Each paper presents information which could be read independently, but contributes to the entire general introduction (chapter 1) and synthesis (chapter 5). The entire dissertation is formed by six chapters.

## 2. CHAPTER TWO

### **Forest, crop and grassland Leaf Area Index estimation using remote sensing: A review of current research trends and accomplishments**

#### **Abstract**

Leaf Area Index (LAI) is an important parameter in plant ecophysiology, it can be used to directly quantify foliage and as a measure of the photosynthetic active area and thus the area subject to transpiration in vegetation. The sensor type (active or passive), model (empirical, physical or hybrid) used to estimate LAI depends on the canopy attributes. The aim of this paper was to review work on remote sensing methods of estimating LAI across different forest ecosystems, crops and grasslands in terms of remote sensing platforms, sensors and models. To achieve this aim, scholarly articles with the title or key words “Leaf Area Index estimation” or “LAI estimation” were searched on Google Scholar and Web of Science with a date range between 2010 and 2020. The results of the study revealed that during the last decade, the use of remote sensing to estimate and map LAI has increased for crops and natural forests. However, with regard to commercial forests and grasslands, there is still a need for more research as the number of studies is still small. Forest ecosystems were broadly grouped into two groups: natural forests and commercial forests, and of the 84 studies related to forests, 60 studies were related to natural studies and 24 studies were related to commercial forests. In terms of model types, empirical models were the most often used models for estimating the LAI of forests followed by physical models. Hybrid models such as PROSAIL were mostly used for crop and grassland LAI estimations. In terms of readily available LAI products, MODIS LAI is the most widely used LAI product.

**Keywords:** LAI estimation, sensors, models, passive, active, data source LAI products

#### **2.1 Introduction**

Leaf Area Index (LAI) is an important parameter in plant ecophysiology, as it can be used to directly quantify foliage and as a measure of the photosynthetic active area and thus the area subject to transpiration in vegetation (Chen, 2013a, Wulder et al., 2004). The importance of LAI is seen in applications ranging from process-based ecosystem simulations, site water balance, and radiative transfer studies. Furthermore, LAI is a major input variable for Physiological Processes Predicting Growth (3PGS) models to predict growth of different species and water use (Waring et al., 2010). LAI estimations and mapping of forests, crop and

grasslands date back to the 1990s. Recent studies of forest, crop and grassland LAIs have been published by Wang et al., (2017), Chen, (2013b), Yan et al., (2019) and Roosjen et al., (2018).

Many definitions of LAI have been proposed in the literature, and these definitions are often dependent on the purpose of the study. For the purpose of this study the following definition will be used: LAI is the total one sided area of leaf tissue per unit ground surface area (Watson, 1947). According to this definition, LAI quantitatively measures the leaf surface area available for the interception of photosynthetically active radiation (PAR) and transpiration, and is an important structural variable for describing the energy and mass exchange in a vegetated ecosystem (Gong et al., 1995b).

There are various methods of measuring LAI, which can be broadly grouped into two categories: direct and indirect methods. Direct methods of estimating LAI include harvesting, litter collection and allometry and are more accurate than indirect methods (Jonckheere et al., 2004). Indirect methods include optical devices such as LICOR-2200, which measures intercepted radiation below the vegetation canopy (Davhula, 2016). Deriving LAI from remote sensing data is another indirect method of estimating LAI. Both these methods of estimating LAI offer different advantages and disadvantages. However, indirect methods have been shown to offer more advantages than disadvantages, especially when a large area is being studied. Remote sensing is one of the commonly used indirect methods of estimating LAI as remote sensing technology offers a better alternative to estimating and mapping LAI for larger landscapes more efficiently and accurately (Pu and Cheng, 2015). Remote sensing also offers a less time consuming and cost effective method of estimating LAI (Xu et al., 2020).

The development of high spatial resolution satellite data has enabled researchers around the world to more effectively monitor vegetation at higher accuracy (Kross et al., 2014). Remote sensing enables convenient collection of data dating back to several years while providing reliable and accurate estimates of LAI and other biophysical attributes for different vegetation types. Although a number of remote sensing methods of estimating LAI have been developed, not a single method can be applied consistently and repeatedly for estimating LAI locally and regionally (Sibanda et al., 2017). The reason for this is variations in biophysical, environmental and topographic traits of vegetation in space and time (Sarker and Nichol, 2011, Bastin et al., 2014)

LAI can be derived by using empirical, statistical and hybrid methods. Deriving LAI by means of statistical and physical approaches was first carried out on crop canopies in the beginning of

the 1970s. One of the earliest studies on estimating LAI using statistical approaches was carried out in 1974 by Kanemasu et al., (1974) who used Landsat MSS to derive wheat LAI. In recent years, the number of studies on crop LAI have been increasing, while recent studies on crop LAI have been published by Kross et al., (2014), Lu and He, (2019), Macedo et al., (2018) and Feng et al., (2019). After research on crop LAI estimations using statistical approaches started showing positive results in the 1980s, the number of forest LAI studies started increasing. With regard to commercial forests and grasslands, there is still a limited number of studies, therefore this area requires further investigation.

During the last decade, the use of remote sensing to estimate and map LAI has increased (Zhou et al., 2014a). High spatial and spectral resolution sensors such as QuickBird, IKONOS and WorldView-3 have shown great potential in achieving acceptable levels of accuracy in estimating LAI. The availability of high spatial resolution sensors such as the ones mentioned above has also led researchers to investigate the effects of spatial and spectral resolution in effectively estimating LAI. In a study conducted by Holmgren and Thureson, (1998) about satellite remote sensing for forestry planning, it was concluded that 30m spatial resolution provides insignificant results when it comes to forest management planning. Gebreslasie and van Aardt, (2011) conducted a similar study as the one mentioned above but used a higher spatial resolution satellite sensor. In this study, forest structural attributes such as diameter at breast height (DBH), mean tree height (MTH) volume and basal area (BA) were investigated for the same species and in the same geographical area but results were different. In terms of coefficient of determination, results were as high as 0.64 for DBH.

Advancements in remote sensing have made it possible to estimate LAI timely with acceptable accuracy. A number of previous studies have estimated LAI with acceptable accuracies using spectral reflectance, however; due to saturation of vegetation indices at LAI values above 3, texture measures have been utilised as an alternative (Gu et al., 2013). Image texture is the measure of the spatial variation in the grey levels in the image as a function of scale. Image texture has been demonstrated by Gu et al. (2013), Pu and Cheng, (2015), Li et al. (2019) to improve the estimation of LAI.

This paper reviews previous work on remote sensing methods of estimating LAI across different forest ecosystems, crops and grasslands. This review looks at the current trends and accomplishments and direction of research in terms of different remote sensing platforms, sensors and models that are utilised to estimate LAI. To achieve this, the paper reviews

published papers on LAIs estimated using remote sensing from the past ten years. Remote sensing has been used by a number of researchers to estimate LAI globally and the availability of different remote sensing imagery and increases in diversity of spatial, spectral, temporal and radiometric characteristics have led to more research and thus better accuracy in estimating LAI (Chen, 2013a).

## **2.2 Materials and Methods**

Scholarly articles with the title or key words “Leaf Area Index estimation” or “LAI estimation” were searched on Google Scholar and Web of Science with a date range between 2010 and 2020. In total, 490 articles were found, 312 were found from Google Scholar and 178 were found on the Web of Science. These articles were downloaded into Endnote (The EndNote Team, 2013), whereafter duplicated articles were discarded. The remaining articles were then filtered to eliminate conference papers, review papers, theses, book chapters, and audio visual material. Studies focusing on LAI estimations using ground based handheld devices and studies focusing on LAI estimations for vegetation cover types of no interest were also removed. This reduced the dataset to 165 journal articles from 23 different journals (Table 2.1). These journal articles were then manually screened to study sites, satellite sensor used, and statistical method used to determine LAI. Of the 168 papers reviewed, 157 used optical devices to estimate LAI data, and only 8 papers measured LAI using ground-based methods.

## **2.3 Results**

A total of 168 journal articles were screened from 23 different journals (Table 2.1). Remote Sensing of Environment had the most publications (38) followed by Remote Sensing (26), International Journal of Remote Sensing (18) and IEEE Transactions on Geoscience and Remote Sensing (10). Journals such as International Journal of Applied Earth Observation and Geoinformation, Agricultural and Forest Meteorology and Canadian Journal of Remote Sensing had less than 10 journal articles while journals such as Journal of Geography, Environment and Earth Science International, Precision Agriculture and Plant Methods had one publication each.

**Table 2.1** Journal list and the number of articles for forest, crop and grassland

<b>Journal</b>	<b>Number of publications</b>
Remote Sensing of Environment	38
Remote Sensing	26
International Journal of Remote Sensing	18
IEEE Transactions on Geoscience and Remote Sensing	10
International Journal of Applied Earth Observation and Geoinformation	9
Agricultural and Forest Meteorology	9
Canadian Journal of Remote Sensing	9
ISPRS Journal of Photogrammetry and Remote Sensing	6
IEEE Journal of Selected Topics in Applied Earth Observations and Remote Sensing	6
Forests	6
GIScience & Remote Sensing	5
Remote Sensing Letters	4
Sensors	4
Journal of Forestry Research	4
Forest Ecology and Management	3
European Journal of Agronomy	2
Chinese Journal of Geophysics	2
Journal of Quantitative Spectroscopy and Radiative Transfer	2
Annals of Forest Science	1
Precision Agriculture	1
Plant Methods	1
Journal of Geography, Environment and Earth Science International	1
Journal of Remote Sensing	1

### 2.3.1 *Application areas*

As mentioned above, this paper reviewed 168 papers related to estimating LAI across different forest ecosystems, crops and grasslands. Forests had the highest number of studies, having had 84 studies, followed by crops with 56 studies and grasslands 25 studies (Figure 2.1). Forest ecosystems were broadly categorised into two groups: natural forests and commercial forests, and of the 84 studies related to forests, 60 studies were related to natural studies and 24 studies were related to commercial forests (Figure 2.2).

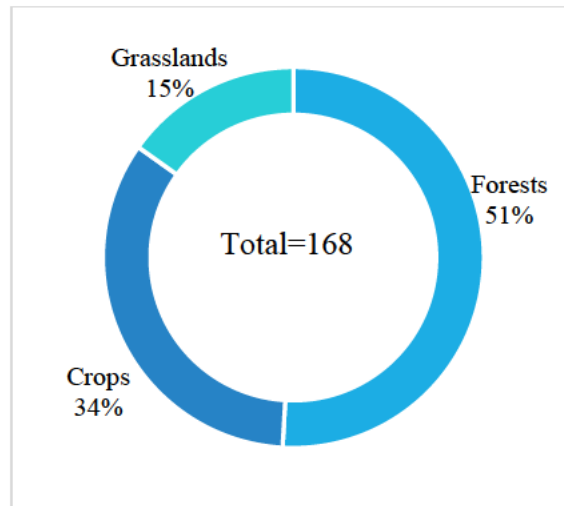


**Figure 2.1** Number of LAI studies for forest, crop and grassland

### 2.3.2 Spatial distribution of LAI studies

Of the 168 studies that were reviewed, 12% were conducted at a global level. At the continental level, North America (12) had the highest number of studies followed by South America (9), Europe (6), Asia (5), Australia (4) and Africa (3) (Figure 2.3). Fourteen studies were conducted at variable levels.

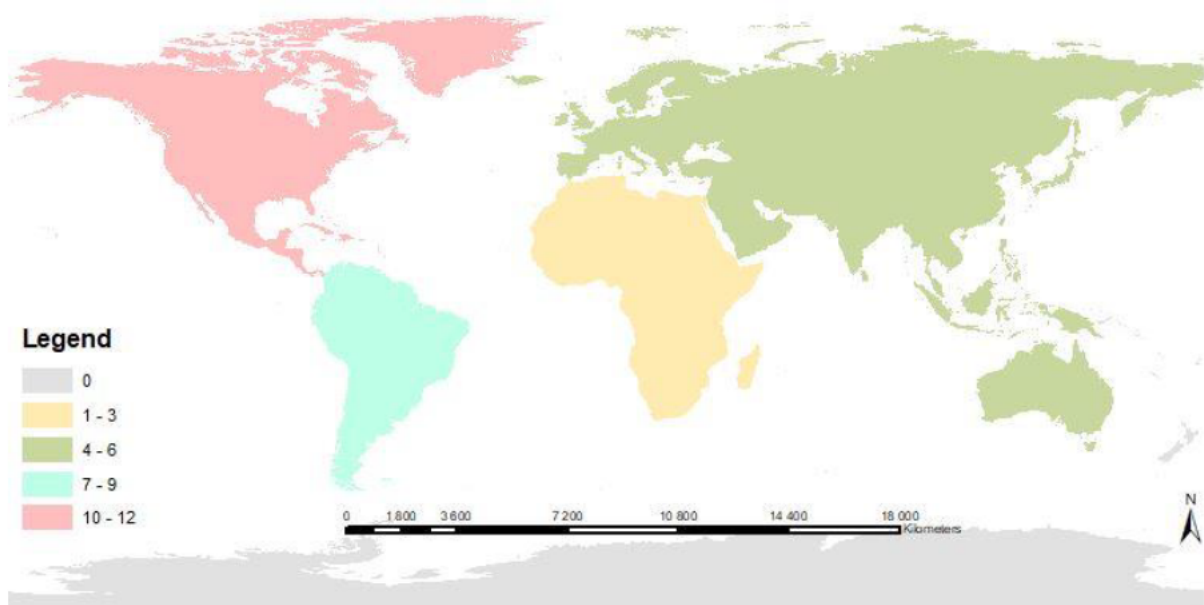


**Figure 2.2** Spatial distribution and number of studies conducted at continental level

The spatial distribution of studies at country and sub country scale shows that China (29) had the highest number of studies followed by the US (21), Brazil (16), Australia and Spain (11)



and New Zealand (10) (Figure 2.4). There were a number of countries in Africa, Asia, South America and the Middle East that had no studies at country scale.

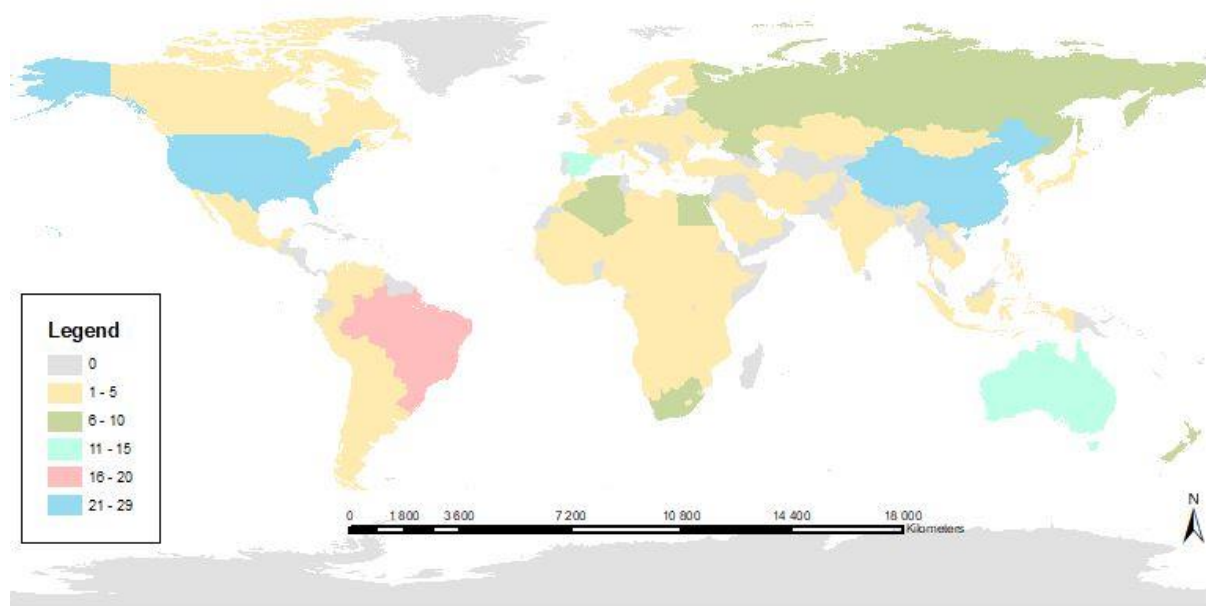


**Figure 2.3** Spatial distribution and number of LAI studies conducted at country level

### 2.3.3 Satellite data used

Advancements in remote sensing technology have enabled researchers around the world to timely and accurately monitor vegetation. According to Lavender (2017), the number of satellite systems for vegetation monitoring has increased by 66% during 2016. Remote sensing enables the convenient collection of data dating back several years while providing reliable and accurate estimates of LAI and other biophysical attributes for different vegetation types.

The majority of forest, crop and grassland studies analysed in this paper used Landsat, followed by Sentinel and MODIS sensors. Freely accessible satellite data such as Landsat, Sentinel and MODIS have gained popularity compared to commercial satellite data sources, such as WorldView, IKONOS and QuickBird. Other commonly used sensors for estimating LAI were WorldView-3, SPOT, QuickBird and IKONOS. LiDAR data was mostly used on forests, followed by crops. There were only four studies on grasslands that used LiDAR data (Figure 2.5). In general, forests have a complex canopy structure, therefore; observing forest parameters using LiDAR has been shown to be efficient (Arnó et al., 2012), especially for reducing the impact of LAI saturation (Hadaś and Estornell, 2016).

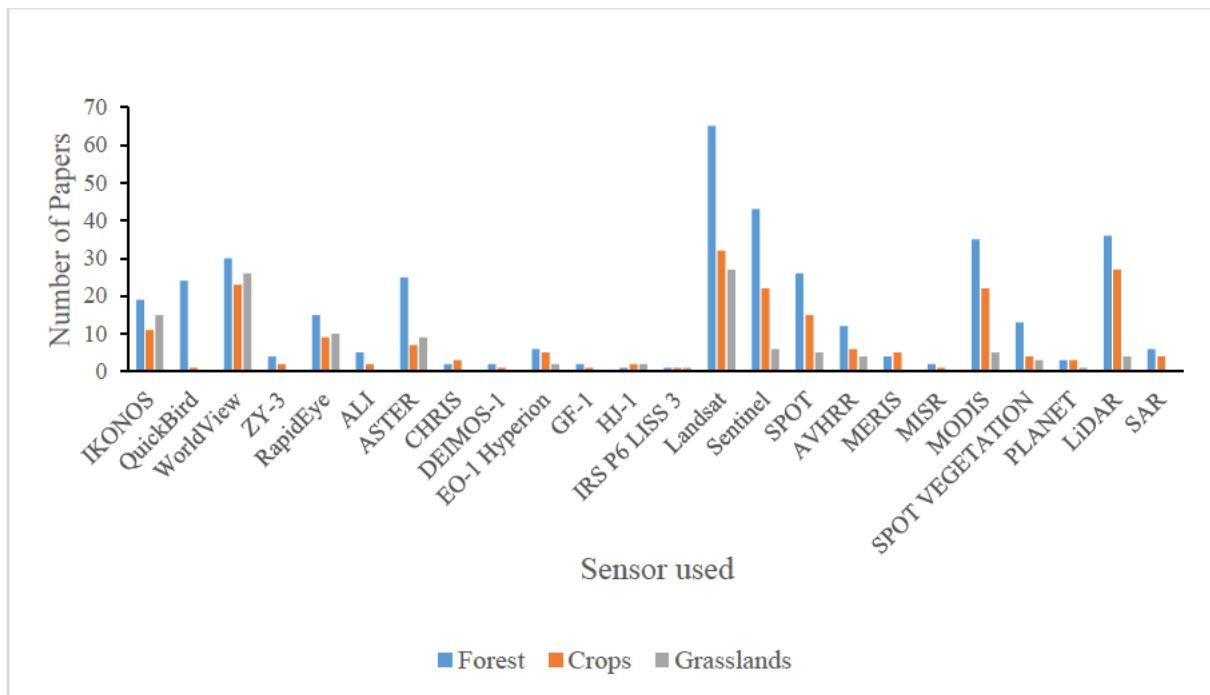


**Figure 2.4** Sensors used to estimate LAI for forest, crop and grassland

Passive sensors are the most widely used sensors for forest, crop and grassland LAI studies. Active and multisource remote sensing had a small proportion of studies. This review showed that the majority of forest and crop studies were carried out using active and passive sensor types, while grassland LAI studies mostly used passive sensors. There were no grassland LAI studies carried out using active remote sensing (Xu et al., 2020). The increase in freely available passive satellite data led to extensive use in forest, crop, and grasslands. The number of LAI estimation studies using passive sensors was three times higher when compared to active remote sensing studies. The number of studies using unmanned aerial vehicles (AUV) has increased since 2010, which has enabled a quick turnaround time and real time crop monitoring. There were a few forest and grassland LAI studies that used AUV compared to crop LAI studies. Figure 2.6 below depicts the application of different sensor systems for forest, crop and grassland studies.

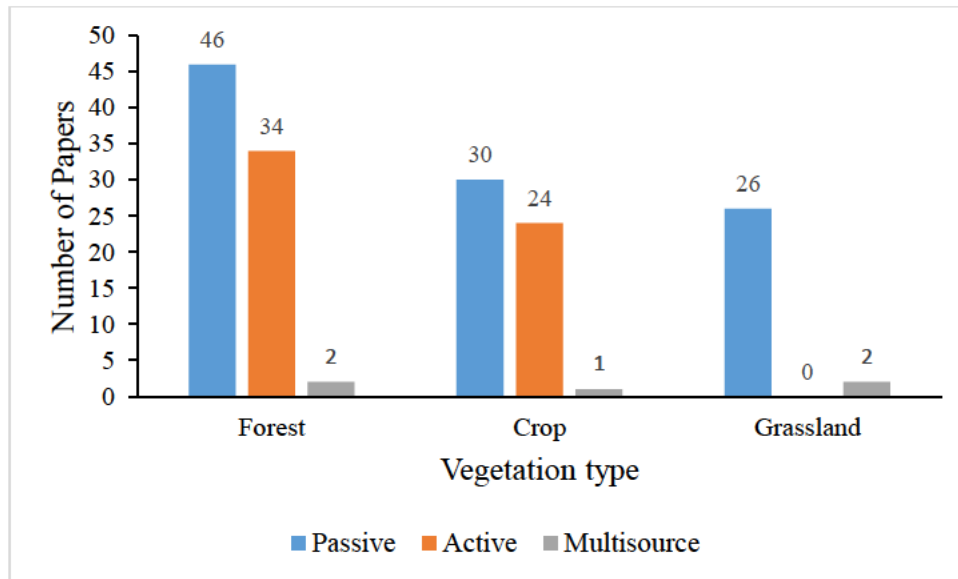


**Figure 2.5** Application of different sensor systems for forest, crop and grassland

In terms of commercial forests, according to the figure 2.6, most forest studies used passive sensors. LiDAR was the most used active remote sensing type for commercial forests. LiDAR is one of the most common active remote sensing systems which detect canopy attributes by emitting light pulses to the target feature, measuring distance ranges and generating three dimensional information about the canopy structure (Lim et al., 2003, Zhao et al., 2015, Zheng and Moskal, 2009). LiDAR is the most commonly used active remote sensing system for forestry (Peduzzi et al., 2012, Luo et al., 2018, Cui et al., 2011), there were fewer crop studies and there were no studies for grasslands that used LiDAR. This may be because discreet LiDAR data tends to have a poor penetration ability in short vegetation.

#### 2.3.4 LAI estimation models used for forest, crop and grassland measures

Figure 2.7 shows the number of forest, crop and grassland LAI studies that used empirical, physical, hybrid and other models. The figure also shows the accuracy range of the methods used in the abovementioned models. To measure model performance,  $R^2$  and RMSE were used. Of the 168 papers that were reviewed, 19 papers applied multiple models with a single data source. In addition, the review has shown that not many studies have used image texture to estimate LAI and therefore requires further investigation.

This review shows that empirical models were the most often used models for estimating the LAI of forest environment from 2010-2020. In terms of physical and hybrid models, forests have a lowest number of studies compared to crops and grasslands. The differences may be

attributed to the typically complex forest structures. The number of crop studies that used physical and hybrid models, particularly PROSIAL, was higher compared to forests and grasslands. In terms of model types, VI based models and reflectance models were the most often applied model types for forests, crops and grasslands. Figure 2.7 shows the number of studies that applied each type of model. The number of applied models is higher than the number of studies reviewed because 19 papers used more than one model.

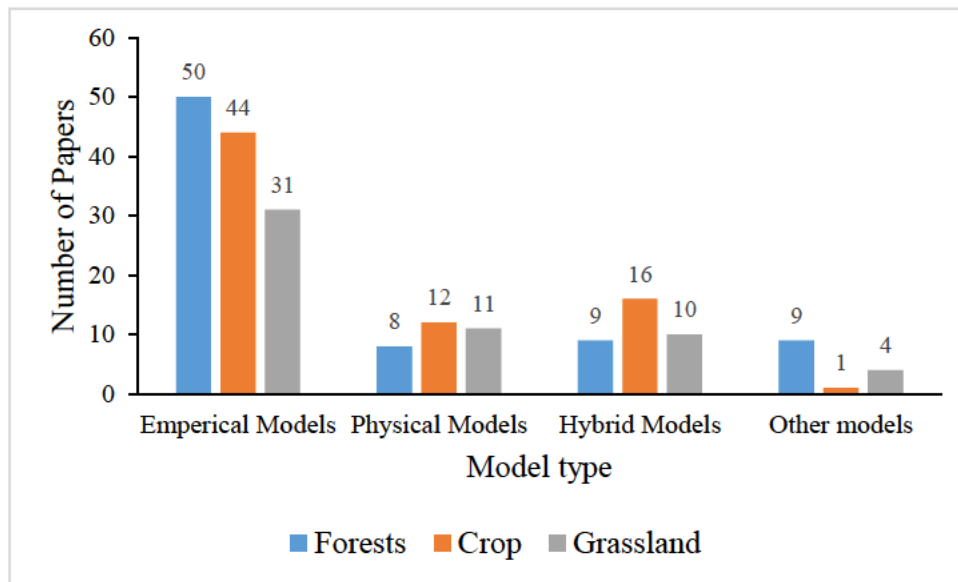


**Figure 2.6** Distribution of different model types for forest, crop and grassland LAI estimations

#### 2.3.4.1 Empirical based models

One of the commonly used remote sensing methods of deriving LAI from spectral data is the empirical-based approach (Campos-Taberner et al., 2016). In this approach regression models are used to study the relationship that exists between the target variables, for example, LAI and its spectral reflectance. Empirical methods also use derived metrics and machine learning methods to derive LAI. The number of studies exploring newly developed VIs and models is increasing for forest, crop and grassland LAI estimations.

The  $R^2$  of empirical models ranged from 0.14-0.99 and the RMSE ranged from 0.01-2.41 (Appendix 3). This indicates that the performance of empirical models is variable. Machine learning methods performed relatively consistently for forest in terms of the  $R^2$  (0.85-0.93). Unlike forests, crops and grasslands had a highly variable performance in terms of  $R^2$  (0.44-0.98). The use of machine learning algorithms for estimating LAI has shown positive results in a number of studies, examples include Lin et al., (2019), Zhang et al., (2011), Omer et al.,

(2016) and Verrelst et al., (2012). A study conducted by Omer et al., (2016), using WorldView-2 imagery demonstrated that machine learning algorithms, such as support vector machines (SVMs) and artificial neural networks (ANN) can accurately predict LAI at tree species level. The SVM model which was based on validation data achieved an  $R^2$  of 0.75. There was an overall increase in machine learning methods, especially for big data calculations.

There are more than 150 vegetation indices that have been developed for mapping and estimating biomass, either using space borne, airborne and ground based sensors (Furniss et al., 2009). Of the 150 vegetation indices, only a few have been tested and validated (Liang et al., 2015). Goswami et al., (2015) estimated LAI and other plant structural attributes using satellite images. This study used traditional vegetation indices such as Normalized Difference Vegetation Index (NDVI) and found that NDVI has a strong correlation of  $R^2 = 0.83$  with biomass and  $R^2=0.70$  with LAI. Although different VIs have shown positive results for estimating LAI, there is no VI that is generic and can be applied consistently and continuously to estimate LAI regionally and globally.

#### *2.3.4.2 Physical models*

Another method of deriving LAI from spectral data is through the inversion of radiative transfer (RT) or physical process models. Radiative Transfer Models (RTM) have been shown in a number of studies as one of the successful methods of estimating LAI from remote sensing data (Liu et al., 2012, Banskota et al., 2013, Le Maire et al., 2011, Su et al., 2019). The widely used and well validated RTMs are PROSPECT, which is a 1-Dimensional leaf reflectance model (Jacquemoud and Baret, 2000) and SAIL, which is a canopy reflectance model (Vohland and Jarmer, 2008). The performance of physical models in terms of  $R^2$  (0.71-0.99) was relatively consistent compared to empirical models (0.14-0.99). Appendix 3 shows key models that were applied in the reviewed papers. The model with the highest number of applications in forest, crop and grassland studies was PROSAIL, which could be attributed to its ease of use and robustness. From the studies that were reviewed in this paper, there were no crop and grassland LAI studies that applied the PROSPECT+DART model, while 4-Scale BRD and DART models had the highest number of applications in forest environments.

Darvishzadeh et al., (2019a) used the combined version of PROSPECT and SAIL known as PROSAIL to retrieve the LAI of saltmarsh from Sentinel-2 and RapidEye satellite data. This study achieved an  $R^2$  of 0.59 and RMSE of 0.16. The adaptability of this model is highly

dependent on the type of remote sensing data, the ecosystem and the texture of the vegetation canopy.

Quan et al., (2017) used the radiative transfer model to estimate the LAI of grasslands. The RTM-based method showed a higher accuracy of  $R^2 = 0.64$  and  $RMSE = 42.67 \text{ gm}^{-2}$  when compared to other models. However, the disadvantages of the RTMs are that they are not as fast as other methods and they have many parameters which are difficult to acquire (Quan et al., 2017).

#### *2.3.4.3 Hybrid models*

Hybrid models combine statistical and RTM input and output data to generate a simulation dataset which includes spectral data, VIs and biophysical and biochemical properties of vegetation (Wei et al., 2017). There are different hybrid model types, which include an iterative approach, optimisation method, look up tables (LUT) and artificial neural networks. In terms of machine learning algorithms, ANN was most prominent type of hybrid model in the reviewed literature; this has gained popularity because of its computational speed and retrieval performance (Verger et al., 2011). ANN has been reported in literature as more accurate than empirical models for estimating LAI (Jensen and Binford, 2004). A number of studies have applied hybrid models and achieved satisfactory results, and these include Verrelst et al., (2012), Qu et al., (2012) and Liang et al., (2015).

The  $R^2$  range of hybrid models was 0.21-0.99 while the RMSE range was 0.26 -1.13. The study by Rivera et al., (2013), compared a hybrid PROSAIL model and empirical model based on NDVI and Simple Ratio (SR), the study found that PROSAIL performed better in terms of RMSE (0.38), while the RMSE of NDVI was 2.28 and 0.88 for SR. Hybrid models can be used to calibrate traditional VIs such as NDVI, develop new VIs and analyse the performance of VIs.

#### *2.3.5 Other LAI Products*

There is a wide range of LAI products available. This section discusses some of the widely used LAI products that were operational after 2010. Advancements in radiative transfer models have facilitated the development of operational global and regional LAI products. Although discrepancies between ground LAI data and digital LAI products still remain, improvements in atmospheric correction and radiometric calibrations have improved LAI retrieval accuracy of many LAI products.



MODIS LAI is one of the most widely used LAI products which is based on biome specific 3dimensional radiative transfer (3D RT) model. This model uses atmospherically corrected reflectance and a biome map to generate retrievals (Le Maire et al., 2011). The MODIS LAI product is derived from the daily MODIS-Terra data and has been available since 2000. Moreover, this data is available daily at 1 km spatial resolution.

There are many other LAI products that have been developed. The Multi-Angle Imaging Spectrometer (MISR) is another LAI product that has been used since 2000. This product is based on the same 3D RTM algorithms as the MODIS product, where the difference between MODIS and MISR is that MISR uses combined spectral data directional information collected by MISR. MISR algorithms provide LAI retrieval for 60-90% of the model input data (Wan et al., 2009).

GEOV2 LAI is another LAI product. This product is a Geoland2/BioPar project. GEOV2 is an improvement of the previous GEOV1 product in terms of continuity. GEOV2 data has less than 1% gaps compared to 20% of missing data/gaps in GEOV1 (Fang et al., 2019), GEOV2 also provides cleaner data that is less affected by radiometric and geometric noise. The data has been freely available since 2000 at the Copernicus portal (<https://land.copernicus.eu/>).

Global Land Surface Satellite (GLASS) LAI dataset was developed by Beijing Normal University and can be accessed at (<http://www.bnu-datacenter.com>). This product has a revisit time of eight days and operated from 1982 to 2012. From 2000 to 2012 the GLASS LAI product was derived using General Regression Neural Networks (GRNNs) from MOD09A1, which is a MODIS land surface reflectance (Liang et al., 2021). This data was available at 1 km for the globe.

GLOBMAP LAI is long term global LAI product which was developed in 1982 through a fusion of MODIS and historical Advanced Very High Resolution Radiometer (AVHRR) data. This product was developed by establishing a simple pixel to pixel relationship between MODIS and AVHRR datasets. This data is available at 8 km resolution.

EPS LAI is a global LAI product generated from AVHRR sensor on board the MetOp (Meteorological–Operational) satellite constellation. This data is available on a 10 day basis from <https://landsaf.ipma.pt/en/>. EPS LAI data is derived from an algorithm that uses the PROSAIL radiative transfer model as input and training data.

PROBA-V LAI is a first version Copernicus Global Land service global LAI product available at <https://land.copernicus.eu/>. This dataset is generated from Sentinel-3/OLCI, PROBAV sensors every five days and the spatial resolution of this dataset is 1/3 km.

The Visible Infrared Imaging Radiometer Suite (VIIRS) LAI dataset is a National Aeronautics and Space Administration (NASA) product. This dataset was developed in 2018 and is still operational. The data can be downloaded at <https://search.earthdata.nasa.gov/search>. The data is available every eight days at a spatial resolution of 500m. The VIIRS LAI dataset can be used to study energy absorption of broadleaves and coniferous vegetation canopies.

## **2.4 Discussion**

This literature review investigated forms of LAI estimations using remote sensing technology for forests, crop and grasslands. The paper further unpacked trends in the use of different sensor systems, models, number of journal articles published and LAI products. The review found that there has been considerable advancements in terms of satellite system technology and models used for LAI and this has led to improvements in LAI index estimation accuracy. Accurate LAI estimates of forests, crops and grassland are essential for improving the management and enhancement of the health of these vegetation types.

There has been great progress in terms of satellite data availability and access since the launch of Landsat in 1972. Easy access to data meant the increase in the number of studies using free satellite data such as Landsat, Sentinel and lower spatial resolution Moderate Resolution Imaging Spectroradiometer (MODIS). Although commercial satellite data is still relatively costly, it offers a better spectral and spatial resolution. The most commonly used commercial satellite data in this review were SPOT, QuickBird, IKONOS and WorldView (Figure 2.5). The popularity of the aforementioned commercial satellite is because of high spatial resolution and higher revisit times. The results also showed an increasing trend in the fusion of data from different sensors and data with different spatial, spectral and temporal resolution.

Of the 168 forest, crop and grassland LAI estimation papers reviewed, the use of passive remote sensing in these studies was almost three times higher when compared to active remote sensing studies. In terms of active remote sensors, LiDAR was more widely used for forests than crops and grassland. These findings are consistent with the previous review paper conducted by Xu et al., (2020) which reviewed research trends and future directions of LAI estimations using remote sensing from 1990 to 2020. Radar systems have been mostly used for crops compared to forests and grasslands. Generally, crops are more dynamic throughout the growing season;



therefore radar systems that function under varying cloud conditions are useful for temporal or time-series crop analysis and can be used even during seasons of high cloud cover. Although grasslands are homogenous and less dynamic throughout the growing season, they usually cover larger areas, which poses a challenge when obtaining and processing data.

Remote sensing studies on LAI for forests, crop and grasslands were conducted across a wide range of scales. Although the majority of studies were conducted at local and sub country scales (110), there were also studies conducted at global (7) continental (19) and country scales (29). There were also 14 studies that were conducted at variable scales. Analysing data of studies conducted at continental or global levels is challenging as it requires high computer processing power.

Empirical, physical and hybrid model types have different advantages and limitations. Empirical models as shown in the results section, are most commonly used models and are effective as they can be used across different data types to determine the relationship between LAI and spectral reflectance data. However, these methods utilise large statistical data inputs and can only be applied at certain locations as they are highly dependent on vegetation types and canopy structural change (Gu et al., 2013). Another limitation of empirical models is saturation problems. Although some studies have shown that this problem can be mitigated by incorporating modified indices, this problem cannot be completely avoided when using optical imagery. According to Thissen et al., (2004), machine learning algorithms have offered a better way to analyse remote sensing data as they do not make assumptions about variable distributions. However, it is important to understand the limitations of empirical methods such as machine learning algorithms (e.g. multi-collinearity) before applying them.

Physical models, unlike empirical models, provide solutions developed without strong reliance on field data (Darvishzadeh et al., 2019b). The great advantage of physical models is their applicability at wide range locations and scales, where they can also be applied to a wide range of vegetation types and canopy structures. The results show that there is an increase in the application of all model types. However, in terms of physical models, PROSAIL is the most commonly used radiative transfer model. A challenge associated with physical models is that they are complicated, as they require many data inputs and are time consuming to process.

Hybrid models are a combination of empirical models including machine learning algorithms, regression methods and physical models. Darvishzadeh et al., (2019b) used the combined

version of PROSPECT and SAIL known as PROSAIL to retrieve the LAI of saltmarsh from Sentinel-2 and RapidEye satellite data. This study demonstrated that RTM is one of the best methods to estimate LAI from remotely sensed data. However, the adaptability of this model is highly dependent on the type of remote sensing data, ecosystem and the texture of the vegetation canopy.

As mentioned in the results section, the current trend for forest, crop and grassland LAI estimation is the exploration of newly developed algorithms based on machine learning methods, especially for big data calculation. However, there are still challenges associated with the use of hybrid models, which include the problem of instability and model overfitting. Problems associated with hybrid models are inherited from empirical models since hybrid models integrate the methods of empirical models.

There are other models which are less frequently reported in literature. These models include the Radiative Transfer (GORT) model (Guijun et al., 2011, Wang and Fang, 2020), Geometric Optical Mutual Shadowing (GOMS) model (Li and Strahler, 1985, Fu et al., 2011), Geometric Optical and a two-layer canopy-reflectance model (ACRM) (Kuusk, 2001, Liu et al., 2016), Kuusk–Nilson forest reflectance model (Nilson et al., 2003, Kuusk et al., 2019) and DART which is a 3D canopy reflectance model developed by (Gastellu-Etchegorry et al., 2004). A review by Song, (2013) concludes that combining new algorithms and complementary information from various sensors leads to the development of better global LAI products.

There are a number of global LAI products that have been developed. For example, MODIS, MERIS, which are medium to coarse resolution data, are most widely used satellite sensors to generate global LAI products. Feng et al., (2019) reviewed the quality of MODIS (MOD15A2), Copernicus PROBA-V (GEOV1), and the recent EUMETSAT Polar System (EPS) LAI products for croplands LAI estimation and found that the quality of LAI data from the abovementioned satellite data is closely related to Sentinel-2 and Landsat 7/8 LAI data ( $R^2=0.90$ ,  $RMSE = 0.50$ ). Other popular LAI products include GEOV2 LAI, Global Land Surface Satellite (GLASS) LAI and GLOBMAP LAI.

The availability of satellite data which combine high revisit time, with high spectral and spatial resolution has fast tracked the development and validation of sophisticated models for LAI estimation. The current focus on improving the robustness of RTMs will lead to the development of even better and more accurate LAI products.

## 2.5 Conclusion

This paper reviewed 168 published articles on LAI estimations for forests, crops and grassland. The paper reviewed articles in terms of study sites, satellite sensors, and statistical methods used to determine LAI. The results of the study indicate that there is an increasing trend in the use of all model types. However, the majority of the literature still focuses on conventional statistically focused empirical models. There is also an increasing trend in the fusion of data from different sources. The fusion of multi-source data includes using data with different spatial, spectral and even temporal resolution. In terms of passive and active sensors, LiDAR demonstrated a great ability to detect forest canopy structures and estimate forest LAI even in mixed species plantations.

The development of high spatial resolution sensors like World View-3 has increased efficiency and improved results drastically. However, like other systems, remote sensing has its drawbacks. One of them is the dependency on weather conditions, as some measurements can only be taken under clear skies conditions. Although a number of remote sensing methods of estimating LAI have been developed, not a single method can be applied consistently and repeatedly for estimating LAI locally and continentally. The reason for this is variations in biophysical, environmental and topographic traits of vegetation in space and time. In the short term, empirical models that can be validated locally are recommended for forest and crop managers.

# 3. CHAPTER THREE

## **Estimating Leaf Area Index of *Eucalyptus dunnii* in Midlands Area, KwaZulu-Natal province over two seasons using vegetation indices and texture measures derived from WorldView-3 imagery.**

### **Abstract**

Leaf Area Index (LAI) remains one of the most important forest structural attributes, as accurate estimations of LAI are crucial, because LAI is a major input variable for Physiological Processes Predicting Growth (3PGS) models to predict growth of different species and their water use. LAI estimation methods are species and location specific therefore there is need for a model for estimating LAI of *Eucalyptus dunnii* in the Midlands, KwaZulu-Natal province of South Africa. Using the Partial Least Squares Regression (PLSR) algorithm, this study investigated three techniques to determine the best technique for estimating LAI using WorldView-3 imagery in the Midlands area. The PLSR texture ratios model achieved the highest accuracy of  $R^2=0.70$ , RMSE 1.21 and  $R^2=0.72$ , RMSE=1.26 for wet and dry seasons, respectively. The PLSR model using a combination of vegetation indices had the lowest estimation accuracy, it achieved an  $R^2$  of 0.59, RMSE= 1.38 in 2019 and  $R^2= 0.60$ , RMSE=1.40 in 2020 on the test dataset. The results of this study provided evidence that image texture ratios can be used to effectively estimate LAI with high accuracy.

**Keywords:** LAI estimation, *Eucalyptus dunnii*, Partial Least Squares Regression, Texture measures, commercial forestry.

### **3.1 Introduction**

Canopy structure is the main feature for monitoring forest ecosystems because interactions with the environmental processes such as net primary production and temperature, occur through the canopy (Weiss et al., 2004). Leaf Area Index (LAI) is one of the most important canopy structures and is a key indicator for forest physiological and biological processes, such as gas and energy

exchange and carbon and water balance at local, regional and global scales (Chason et al., 1991). LAI can be defined as the total one sided area of leaf tissue per unit ground surface area (Waring et al., 2010). According to this definition, LAI is the quantity of potential photosynthetic active area in a habitat.

Since LAI is an indicator for vegetation physiological and biological processes, it can be used to reliably monitor forest plantations, thus enabling early detection of forest damage caused by water stress, insect diseases and nitrogen deficiencies. Furthermore, the availability of information about crop health and development can provide forest managers with valuable information allowing for early yield forecasting (Groten, 1993, Mkhabela et al., 2011), efficient fertilizer application (Scharf and Lory, 2002) and weed control (Mahlein et al., 2012, Luedeling et al., 2009).

LAI can be measured through direct and indirect methods. Direct methods include field observations, surveys and litter harvesting, however, these methods are time consuming, costly, laborious and logistically impractical, particularly within large spatial extents (Omer et al., 2016, Yu et al., 2019, Wang et al., 2019). Nevertheless, direct methods are highly accurate and can be used as a reference for the development and improvement of data collected through indirect methods (Cutini et al., 1998). Indirect methods, on the other hand, include innovative approaches such as using vegetation indices obtained through remote sensing, which can generate spatially explicit information on species. This is particularly important within a commercial forestry landscape (Peltzer et al., 2015).

The recently developed high resolution multispectral sensors like WorldView-3 have demonstrated great capabilities in estimating and mapping the LAI of forest species. WorldView-3's unique technical properties such as eight spectral bands and a finer spatial resolution of 1.24m across the visible and near infrared (NIR) regions have proved effective in monitoring forest attributes. These bands are highly sensitive to the variability within forest attributes (Peerbhay et al., 2013). WorldView-3 sensors offer unique imaging bands such as the red-edge band, which is valuable for mapping and distinguishing vegetation attributes. The spatial resolution is one of the most important technical aspects of satellite sensors and it plays a key role in retrieving data about vegetation. In a study conducted by Holmgren and Thuresson (1998) on satellite remote sensing for forestry planning, it was concluded that a low 30m spatial resolution provides insignificant

results in forest management planning. This indicates that it is very important to consider sensor spatial resolution when conducting a forest related study.

*Eucalyptus dunnii* is one of the dominant commercial tree species in the Midlands area of KwaZulu-Natal, South Africa. More than 30% of the Mondi planted area in Greytown is planted with *Eucalyptus dunnii*. So, there is a need to develop an operational method of calculating LAI over a large area such as the Midlands. Moreover, a means of remotely obtaining LAI over a larger area is sought after by many forestry companies. Therefore, this study aims to provide an operational method of efficiently calculating LAI over a large area. This study derived LAI using satellite images, which will be particularly useful to forestry companies that manage landholdings of regional scales. As noted by Gao et al., (2014) the coarse scale LAI products derived from Moderate Resolution Imaging Spectrometer (MODIS) are not adequate or suitable for compartment scale analysis as most Eucalyptus plantations in South Africa contain very few, or no homogenous pixels.

Several studies (Li et al., 2019, Pope and Treitz, 2013, Pu and Cheng, 2015, Lottering et al., 2018) have been conducted using high resolution sensors with reliable accuracy in forestry. These studies are species and location specific and were conducted on a limited landscape. These limitations create the need to develop a model for estimating LAI of *Eucalyptus dunnii* in the Midlands area. To the best knowledge of the researcher, no study has been conducted in South Africa to determine the extent of additional remote sensing techniques in improving the estimation of LAI of *Eucalyptus dunnii*. Therefore, this study aims to determine whether image texture ratios derived from high-resolution WorldView-3 imagery can improve LAI estimation for *Eucalyptus dunnii* in the Midlands area for two different seasons. The objectives included: (1) establishing whether image texture ratios improved the estimation of LAI of *Eucalyptus dunnii* over single texture bands and vegetation indices using the partial least squares regression (PLS-R) algorithm and (2) to map the spatial distribution of LAI over the two seasons using the optimal model and PLS-R.

## 3.2 Study Area

### 3.2.1 Introduction-general description of the study area

This study was conducted within Mondi commercial plantations located in the Midlands area, KwaZulu-Natal. The Midlands area is known for its mountains, hilly and undulating veld and flat surfaces. The Midlands is also popularly known for its warm temperatures and a mean annual temperature of approximately 23°C and high summer rainfall reaching  $\pm 1029$ mm, which is favourably important for fast growth of *Eucalyptus dunnii* (Dube et al., 2014, Dube and Mutanga, 2015)

This study investigated *Eucalyptus dunnii* compartments which are managed for pulpwood production. The study sites were selected to represent a wide range of productivity classes as measured by site indices at reference age of eight years to provide an estimation of LAIs operational at sites of different productivity. Sixteen compartments representing different age classes were selected for this study (Table 3.1) and the ages of the selected compartments ranged from one year to ten years. These compartments were further grouped to represent three phenology periods of *Eucalyptus dunnii*. The ages representing these periods are:

- 1) 1.8 to 3.6 - Canopy closure period
- 2) 4.3 to 6.3 - Mid rotation
- 3) 7.4 to 10.8 - End of rotation

**Table 3.1** General descriptions of study sites

COMPARTMENT	AREA (ha)	AGE (Years)	SITE_INDEX (m)	ESP1 (m)	ESP2 (m)	PSPH
E024	6.7	1.8	26.9	3	2.5	1333
F021	23.9	2.2	22.2	3	2.5	1333
A006	34.3	3.6	20.7	3	2	1666
D016	39.1	4.3	21.1	3	2	1666
C030	17.5	4.8	20.2	3	2	1666
D036	38.9	4.8	17.8	3	2	1666
D021	10.9	5.3	17.8	3	2	1666
D010A	47.1	6.3	21.1	3	2	1666
A001	16.6	7.4	20.7	3	2	1666
D001	17.2	7.7	21.1	3	2	1666
A005	28.9	7.7	17.4	3	2	1666
B015	29.8	8.8	23	3	2	1666
F043	17.7	9.3	20	3	2	1666
B001	26.3	10.3	19.5	3	2	1666
B003	22	10.5	19.5	3	2	1666
A011	7.6	10.8	17.4	3	2	1666

In this study, direct and indirect field based LAI measurements were carried out. Sampling plots in compartments representing age classes were placed in such a way that each compartment would have one sampling plot per one hectare grid. The one hectare grid was created using an ArcGIS sampling tool. Within the one hectare grid, a circular plot of 250sqm was placed using slope and aspect as strata. All compartments were greater than six hectares in size. All sampling plots were uniform in size and they were sampled the same way. Conditions of understory vegetation, uniformity of canopy and tree condition were carefully considered during the site selection process. All compartments with signs of disease infestation, growth loss due to drought and fire scars were excluded from the selection. In addition to this, compartments were inspected through Google Earth's latest image and they were later visited for an infield inspection. Figure 3.1 depicts



the study area. Figure 3.2 depicts the workflow of the methodology undertaken to meet the objectives of this study.

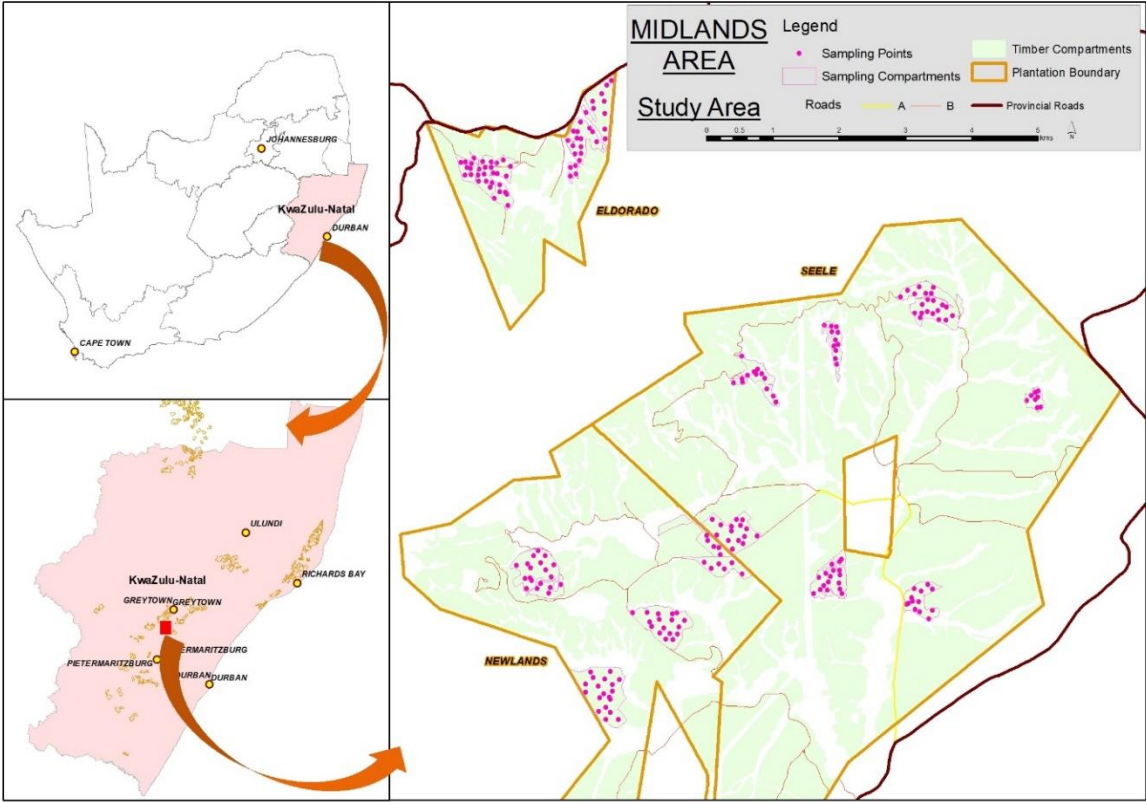


**Figure 3.1** Map of the study area

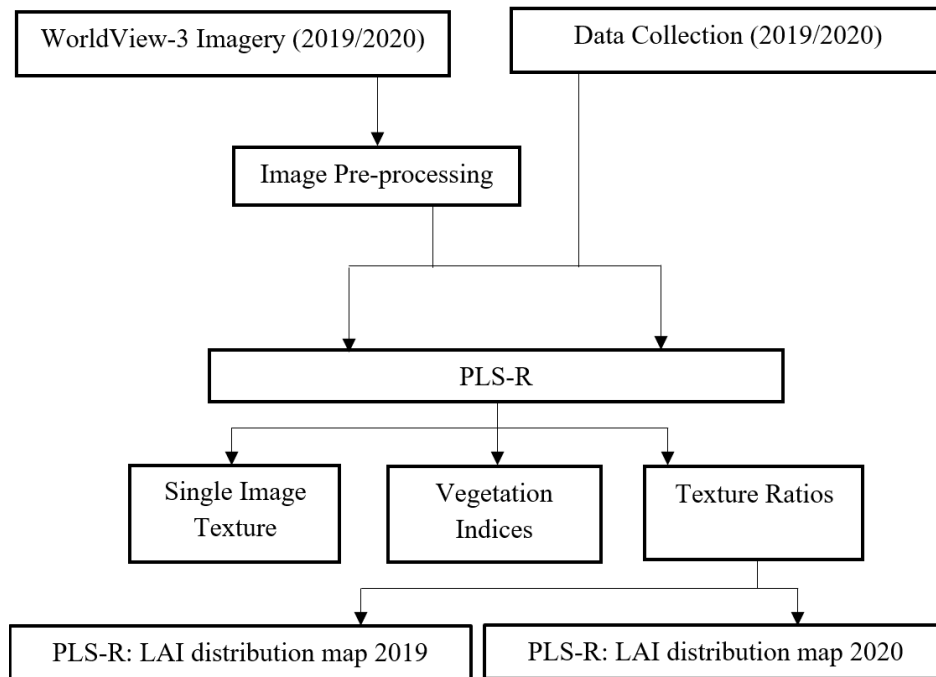


Figure 3.2 Workflow of the methodology undertaken to meet the objectives of this study

### 3.3 Data collection

#### 3.3.1 Destructive sampling

Sampling plots were selected from compartments representing different age groups. In each compartment, three trees representing mean DBH for the compartment were felled at ground level with a chainsaw. Height and crown width of these trees were also measured. DBH for all the trees in the sampling plots were measured at 1.3 m above ground prior to destructive sampling. This method was adapted from (Ghebremicael, 2003) and modified. All leaves were harvested from live branches and put into a box and a 30% subsample of leaves was then taken and placed into paper bags of known weight. The 30% subsample leaves were used for the determination of specific leaf area (SLA) from which LAI was calculated. The subsample was taken to the laboratory where it was measured and oven dried for 72 hours at 60 °C. A desiccator was used to cool dry leaves and prevent absorption of moisture by leaves. Dry leaves were then measured as soon as possible to prevent moisture absorption and determine accurate dry sample weight.

Other tree components such as the stem and live branches were also sampled and measured. Tree stems were cut into 1 m logs and at every one metre crosscut a 3 cm disk was sampled. These discs

were measured with and without bark to determine wood density and volume. Live and dead branches were cut using a garden pruner and separated. Dead branches were discarded and all live branches were weighed in the field while they were still fresh using a 30 kg spring balance scale with an accuracy of  $\pm 0,1$  g.

### 3.3.2 Leaf area determination

The subsample leaves were scanned using an LI-3100 leaf area meter and oven dried. The leaf area meter was calibrated to an accuracy of  $0.1\text{mm}^2$ . To calculate specific leaf area (SLA) from the sub sample, a ratio of oven dry to fresh weight was calculated and an average ratio determined. The SLA which was used to relate dry foliage weight to Leaf Area (LA) was obtained using the equation:

$$\text{SLA (mm}^2\text{g}^{-1}) = \text{LA (mm}^2\text{)/Leaf dry matter (g)....(1)}$$

The tree LA was calculated from SLA using the equation:

$$\text{Leaf area (m}^2\text{) = Tree dry leaf weight (kg) x SLA (m}^2\text{/kg)....(2)}$$

The LAs were then scaled up to the entire plots and then to per hectare volume, as Table 3.2 depicts.

**Table 3.2** Example of destructive sampling data

Compt	Age	Tree No.	Dbh	Height	WF_wet	Sample_WF_wet	Sample_WF_dry	Sample leaf area	Area/tree	Leaf area Tree	LAI	SLA	SLA	Sample
			cm	m	kg	kg	kg	cm <sup>2</sup>	m <sup>2</sup>	m <sup>2</sup>	m <sup>2</sup> /m <sup>2</sup>	cm <sup>2</sup> /kg	m <sup>2</sup> /g	%
A011	10.8	1	16.2	23.42	3.942	1.183	0.669	51213.88	6	17.07	2.844	76.55	7.655	0.30
A011	10.8	2	16.3	25.66	4.471	1.341	0.604	32901.025	6	10.97	1.828	54.47	5.447	0.30
A011	10.8	3	16.6	25.6	4.865	1.46	0.658	37141.287	6	12.38	2.063	56.45	5.645	0.30

### 3.3.3 LiCor-2200 plant canopy analyser

A LiCor-2200 plant canopy analyser was used to measure field LAI or effective LAI. The LiCor-2200 instrument was used in several studies and it has provided reliable LAI estimates. The instrument measures diffuse radiation from different parts of the sky using a fisheye optical sensor with 148° field of view. The sensor comprises five detectors that are placed in concentric rings. The ratio of below-canopy and above-canopy radiation, measured for the five zenith angles,

corresponds to the transmittance of the gap frequency. Estimations of LAI are based on the inversion of the standard Poisson model of gap frequency distribution (Ilangakoon et al., 2015).

All readings were taken under clear skies or uniformly overcast conditions. To eliminate the effect of direct radiation on the sensor, readings were taken facing the opposite direction from the sun. The LAI-2200 sensor can view a full 360° of azimuth, but there are view restrictor masks which restrict the sensor field of view to 270°, 180°, 90°, and 45° which can be attached onto the sensor head to restrict the view of the sensor for purposes such as hiding unwanted objects and features from the sensor view to reduce errors, or to study canopies with leaves asymmetrically distributed about the azimuth. In this study, a viewing restrictor of 180° was used.

Two LI-COR LAI-2200 Plant Canopy Analyser sensors with a 180° viewing cap and one data logger were used to take below and above canopy radiation measurements. On each tree, three below canopy readings were taken around the diameter of the tree. The sensor was held at approximately 1.3 m above the ground. One LAI-2200 sensor was set up in an open area where there was no edge effect but as close as possible to the sampling plots where below canopy readings were taken. The above canopy sensor was set to automatically log readings at 15 second intervals for the duration of plot measurements. A similar approach was followed by Lottering et al., (2018). For a better correlation with direct or destructive sampling readings, three upper rings of LAI 2200 were used to estimate LAI (Kross et al., 2014). Measurements on sloping terrain were made with the sensor parallel to the ground at the same compass direction rather than level. The mean LAIs of stand were calculated by averaging the readings from all sampling plots. LAI readings from each sampling plot were used to determine the within compartment distribution of LAI.

#### *3.3.4 Remote sensing data acquisition and processing*

WorldView-3 images are useful for studying vegetation attributes (Sibanda et al., 2017), and have been used in a number of vegetation health and LAI studies with acceptable accuracy. For the aforementioned reasons, WorldView-3 (WV-3) images were used in this study to estimate LAI. For the wet seasons, a multispectral WorldView-3 image was acquired on 26 September 2019 and for the dry season, another multispectral WorldView-3 image was acquired on the 12 July 2020. Both images have a spatial resolution of 1.24m for multispectral bands and 31cm for the panchromatic bands. Each image consist of eight bands, as shown in Table 3.3.

**Table 3.3** WorldView-3 bands

<b>Band name</b>	<b>Band number</b>	<b>Band width</b>
Coastal Blue	1	397nm-454nm
Blue	2	445nm-517nm
Green	3	507nm-586 nm
Yellow	4	580nm-629 nm
Red	5	626nm-696 nm
Red Edge	6	698nm-749 nm
Near Infrared 1	7	765nm-899 nm
Near Infrared 2	8	85nm7-1039 nm

Image processing was conducted for WV-3 images in ENVI 5.6 software. Image processing included geometric, radiometric and atmospheric correction. Geometric correction and orthorectification of the images were performed by collecting 167 ground control points using a digital elevation model (DEM) with 5m contours. The image was then radiometrically corrected to top of the canopy reflectance and to remove the influence of atmospheric effects (clouds and noise) using the Fast Line of Sight Atmospheric Analysis of Spectral Hypercubes (FLAASH).

### 3.3.5 *Vegetation Indices extraction*

A total of 22 vegetation indices were selected for evaluation. These indices use a combination of the visible, red edge and near infrared bands (Table 3.4). The selected vegetation indices include NDVI, SAVI, and EVI, SR, red-edge normalized difference vegetation index (NDVI<sub>re</sub>), Red Edge simple ratio (SR<sub>re</sub>), Green Difference Vegetation Index (GDVI), MCARI and MTVI2. Vegetation indices can serve as a proxy for LAI and several studies have investigated the actual relationship between LAI and VIs. One such study was conducted by Potithev et al., (2010) in a deciduous broadleaf forest and the results concluded that (1) NDVI and EVI can depict seasonal variations of LAI, (2) NDVI and EVI have a linear relationship with LAI and (3) when combined, NDVI and EVI can improve LAI estimations. However, some studies have reported that the relationship between LAI and NDVI usually saturates under dense canopies (Baret and Guyot, 1991, Gitelson,

2004, Feng et al., 2019). To address this limitation, different VIs have been developed by modifying NDVI through wavelength optimisation or the incorporation of a coefficient (Huete et al., 2002, Inoue et al., 2008, Feng et al., 2019). Replacing the red band in traditional NDVI with bands such as red edge improved the relationships of modified NDVI and LAI (Liang et al., 2015, Fang et al., 2013, Feng et al., 2019). The modified VIs such as the Green NDVI and Normalized Difference Red Edge (NDRE) have been reported in several studies to weaken saturation and thus improve LAI prediction accuracy (Tian et al., 2011, Tillack et al., 2014, Viña et al., 2015, Sun et al., 2020). The 23 VIs were calculated using ENVI 5.6. They were then extracted into a spreadsheet using ArcGIS Pro 2.8.0 zonal statistics tool.

**Table 3.4** Vegetation indices used in this study

Vegetation Index	Acronym	Equation	Environmental Features	Reference
Normalized Difference Vegetation Index	NDVI	$\frac{\text{NIR} - \text{Red}}{\text{NIR} + \text{Red}}$	Chlorophyll and canopy leaf area.	(Rouse et al., 1974)
RedEdge NDVI	RedEdge	$\frac{\text{NIR} - \text{RedEdge}}{\text{NIR} + \text{RedEdge}}$	Chlorophyll and canopy leaf area.	(Gitelson and Merzlyak, 1994)
Simple Ratio	SRI	$\frac{\text{NIR}}{\text{RED}}$	Chlorophyll and LAI	(Jordan, 1969, Rouse et al., 1974)
Enhanced vegetation Index	EVI	$2.5 \frac{(\text{NIR} - \text{Red})}{\text{NIR} + 6 * \text{Red} - 7.5 * \text{Blue} + 1}$	Chlorophyll and LAI	(Huete et al., 1997)
Red green ratio	RGR	$\frac{\text{Red}}{\text{Green}}$	Chlorophyll	(Gamon and Surfus, 1999)
Difference vegetation index	DVI	$\text{NIR} - \text{RED}$	Chlorophyll and LAI	(Tucker, 1979)
Atmospherically resistance vegetation index	ARVI	$\frac{\text{NIR} - \text{Red}}{\text{NIR} + \text{Blue}}$	Chlorophyll	(Kaufman and Tanre, 1996)
Anthocyanin reflectance index	ARI 1	$\frac{(1)}{\text{Green}} - \frac{(1)}{\text{Red edge}}$	Anthocyanins	(Gitelson and Chivkunova, 2001)
Green atmospherically resistant index	GARI	$\frac{\text{NIR} - [\text{Green} - \gamma(\text{Blue} - \text{Red})]}{\text{NIR} - [\text{Green} - \gamma(\text{Blue} - \text{Red})]}$	Chlorophyll	(Gitelson et al., 1996)
Green difference vegetation index	GDVI	$\text{NIR} - \text{Green}$	Chlorophyll	(Sripada et al., 2006)
Visible atmospherically resistant index	VARI	$\frac{\text{Green} - \text{Red}}{\text{Green} + \text{Red} - \text{Blue}}$	Chlorophyll	(Gitelson et al., 2002)
Plant senescence reflectance index	PSRI	$\frac{\text{Red} - \text{Blue}}{\text{Red edge}}$	Chlorophyll and carot-enoids	Merzlyak <i>et al.</i> (1999)
Green normalized difference vegetation index	GNDVI	$\frac{\text{NIR} - \text{Green}}{\text{NIR} + \text{Green}}$	Chlorophyll and LAI	(Ahamed et al. 2011)
Transformed difference vegetation index	TDVI	$\sqrt{0.5 + \frac{\text{NIR} - \text{Red}}{\text{NIR} + \text{Red}}}$	Chlorophyll and LAI	(Bannari et al. 2002)
Soil adjusted vegetation index	SAVI	$\frac{1.5 * (\text{NIR} + \text{Red})}{(\text{NIR} + \text{Red} + 0.5)}$	Chlorophyll	(Huete 1988)
Datt/Maccioni index	DMI	$\frac{\text{NIR} - \text{RedEdge}}{\text{NIR} - \text{Red}}$	Chlorophyll	(Maccioni et al. 2001)
RedEdge yellow ratio	REY	$\frac{\text{RedEdge} - \text{Yellow}}{\text{RedEdge} + \text{Yellow}}$	Chlorophyll	Gwata 2012)

Red edge triangular vegetation index (core only)	RTVIcore	$100(\text{NIR} - \text{REdEdge}) - 10(\text{NIR} - \text{GREEN})$	Chlorophyll and LAI	(Chen et al. 2010)
Modified triangular vegetation index	MTVI	$\frac{1.5[1.2(\text{NIR} - \text{Green}) - 2.5(\text{RED} - \text{GREEN})]}{\sqrt{[2\text{NIR} + 1]^2 - (6\text{NIR} - 5\sqrt{(\text{RED})}) - 0.5}}$	Chlorophyll	(Haboudane et al. 2004)
RedEdge simple ratio	SRre	$\frac{\text{NIR}}{\text{RedEdge}}$	Chlorophyll	(Gitelson & Merzlyak 1994)
Green ratio vegetation index	GRVI	$\frac{\text{NIR}}{\text{Green}}$	Chlorophyll	(Sripada et al. 2006)
Leaf Chlorophyll Index	LCI	$\frac{\text{NIR} - \text{RedEdge}}{\text{NIR} + \text{Red}}$	Chlorophyll	(Gobron et al., 2000)
Green Leaf Index	GLI	$\frac{2 * \text{Green} - \text{Red} - \text{Blue}}{2 * \text{Green} + \text{Red} + \text{Blue}}$	Chlorophyll	(Raymond Hunt Jr. et al., 2011)

### 3.3.6 Texture parameters

Texture parameters are commonly used to measure the spatial variations in the grey levels in the image as a function of scale (Pu and Cheng, 2015). The variations in image texture can result from changes in species type, canopy closure and stem density. Several studies have shown that grey-level co-occurrence measures (GLCMs) can measure and estimate target forest structural attributes (e.g. Hlatshwayo et al., 2019, Pu and Cheng, 2015, Lottering et al., 2018). In this study, GLCMs were applied to study their ability to estimate forest LAI. A total of eight 2<sup>nd</sup> order grey level statistical texture-based features were extracted from the eight WV-3 multispectral images on per band basis (Table 3.5). The selected texture feature measures were relevant to the study and they were selected based on the literature review and their potential for estimating and mapping forest structural attributes including LAI from high resolution MS data, which has been demonstrated in many existing studies (e.g. Gebreslasie and van Aardt, 2011, Gu et al., 2013, Kraus et al., 2009, Murray et al., Zhou et al., 2014b, Ozdemira and Karnielib, Ozdemira and Karnielib, 2011)

The eight texture measures; namely mean, variance, entropy, correlation, contrast and second moment were calculated using 3x3 and 5x5 moving window sizes. These window sizes were selected because they cover a range of sizes that roughly match the spaces between the uniform areas of the canopy in the forest compartment.



**Table 3.5** Texture measures used in this study

Parameter	Equation	Description
Contrast	$\sum_{i,j=0}^{M-1} P_{i,j}(1-j)^2$	Measures the level of local variation within a window(Kayitakire et al., 2006)
Correlation	$\sum_{ij=0}^{M-1} P_{i,j} \left[ \frac{(i - \mu_i)(i - \mu_j)}{(\sigma_i^2)(\sigma_j^2)} \right]$	Measures the grey level linear dependency within an image(Yuan et al., 1991)
Dissimilarity	$\sum_{ij=0}^{M-1} P_{ij}  i - j $	Measures local variation(Rubner et al., 2001)
Homogeneity	$\sum_{ij=0}^{M-1} \frac{P_{ij}}{1 + (1 - j)^2}$	Measures the smoothness of image texture(Tuttle et al., 2006)
Mean	$\mu_i = \sum_{i,j=0}^{M-1} i (P_{ij})$	This is the average grey level in the small neighbourhood(Materka and Strzelecki, 1998)
Second Moment	$\sum_{ij=0}^{M-1} P_{ij}^2$	Indicator of local homogeneity(Yuan et al., 1991)
Variance	$\sigma_i^2 = \sum_{ij=0}^{M-1} P_{ij} (i - \mu)^2$	Variability of the spectral response of pixel(Materka and Strzelecki, 1998)
Entropy	$\sum_{i,j=0}^{M-1} P_{ij} (-\ln P_{i,j})$	This is a statistical measure of uncertainty(Yuan et al., 1991)

The texture parameters found in Table 3.5 and derived from WV-3 images were processed in two steps:

1. The single texture parameters derived from WV-3 images were tested in estimating *Eucalyptus dunnii* LAI using PLSR; and
2. The two band texture ratios derived from WV-3 images and their accuracy in predicting *Eucalyptus dunnii* LAI were assessed using PLSR. It should be noted that ratios were only used for texture parameters that were computed from the same spectral band and moving window. These image texture ratios were derived using the following equation:

$$\text{Image texture} = \frac{B1}{B2} \dots (3)$$

Where B1 and B2 are texture parameters

The equation displays texture parameters, which are rationally combined to form texture ratios for estimating LAI.

### **3.4 Statistical Analysis**

The relationships between LAI and vegetation indices (VI), and LAI and texture were modelled using Partial Least Squares Regression (PLS-R). PLS-R is a data compression technique that is used to create predictive models from data containing highly collinear variables or factors (Chin, 1998 , Haenlein and Kaplan, 2004, Wold, 1996). PLS-R reduces explanatory (X) variables into a few non-correlated latent variables based on the information contained in the response variable(Y), then regresses the new variables against the response variable to build a linear model as follows:

$$Y = X\beta + \varepsilon \dots (4)$$

Where Y is a mean-centred vector of a dependent variable, X is a mean-centred matrix of independent variables,  $\beta$  is a matrix of regression coefficients, and  $\varepsilon$  is a matrix of residuals. Several studies have demonstrated that PLSR is able to extract significant variables and build a reliable model (Hansen and Schjoerring, 2003, Kiala et al., 2017, Abdel-Rahman E.M et al., 2014)

In this study, the leave-out-one cross validation method was used to select the optimal number of components for each PLS-R model. For the development of models, only the number of components with lowest error were selected, this was done to avoid overfitting the models. The ‘plsR’ function in the R statistical software package version 3.1.3 (Team., 2015) was used in this study. It subsequently used the variable of importance in the projection (VIP) method for variable selection as PLS-R does not specify which variables will play the most significant role in the development of the model. VIP methods calculate the significance scores of each vegetation index by ranking its importance among explanatory variances. It is important to incorporate VIP for variable importance because, it increases the robustness of the model development process. All variables with a VIP Score greater than 1 (one) were considered significant and were selected for developing PLS-R models.

### **3.5 Accuracy Assessment**

Model performance was based on an independent test dataset, which was accomplished utilizing the coefficient of determination ( $R^2$ ) and root mean square error (RMSE). The dataset ( $n = 202$ )

was split into 30% test ( $n = 61$ ) and 70% training ( $n = 141$ ) data. Models that had the highest  $R^2$  and lowest RMSE were reserved for estimating LAI. See equation (5) for calculating the RMSE.

$$RMSE = \sqrt{\frac{SSE^2}{n}} \dots (5)$$

Where SSE is sum of errors (observed-predicted values) and n is the number of pairs

### 3.6 Results

#### 3.6.1 Descriptive Statistics

In total, 202 points were used to develop the model. Table 3.6 below shows the number of samples collected, maximum, minimum and average LAI across the study area for the wet and dry seasons. The average LAI was 3.28  $m^2/m^2$  and 2.48  $m^2/m^2$  for wet and dry seasons respectively. Table 3.6 shows a summary of LAI values for the two seasons.

**Table 3.6** Descriptive statistics for LAI values ( $m^2/m^2$ ) measured through LiCor-2200 plant canopy analyser

	Number of points	Maximum LAI	Minimum LAI	Average LAI
<b>Wet season 2019</b>	202	6.06	1.03	3.28
<b>Dry season 2020</b>	202	4.91	1.00	2.48

Direct field LAIs were collected to provide a reference for LAI collected indirectly through a LiCor-2200 plant canopy analyser (Appendix 1). To determine LAI, 45 trees were sampled across the study area. As has been stated in the previous chapter, to calculate LAI from direct field data, Leaf Area (LA) was calculated from SLA and total dry mass, then scaled up to determine LAI for the sampling plot. The average LAI was 2.95  $m^2/m^2$ . Table 7 shows a summary of LAI, SLA and LA values. Appendix 2 shows values for all 45 sampled trees.

**Table 3.7** Descriptive statistics for direct field-based LAI, Specific LAI and Leaf Area

	Number of trees	Maximum LAI	Minimum LAI	Average LAI
<b>LAI(<math>m^2/m^2</math>)</b>	45	5.68	1.09	2.95
<b>SLA(<math>m^2/kg</math>)</b>	45	13.19	5.11	7.40

Leaf Area (m <sup>2</sup> )	45	35.21	6.59	18.13
-----------------------------	----	-------	------	-------

A comparative analysis was conducted to assess differences in LAI between the wet season (2019) and dry season (2020). The results show that LAI values differed greatly between the two seasons with wet season LAI higher than dry season LAIs, indicating that seasonality has a significant influence on LAI. The period of high temperature and high precipitation is associated with higher LAI. Figure 3.3 below represents distributions of LAI values for 2019 and 2020.

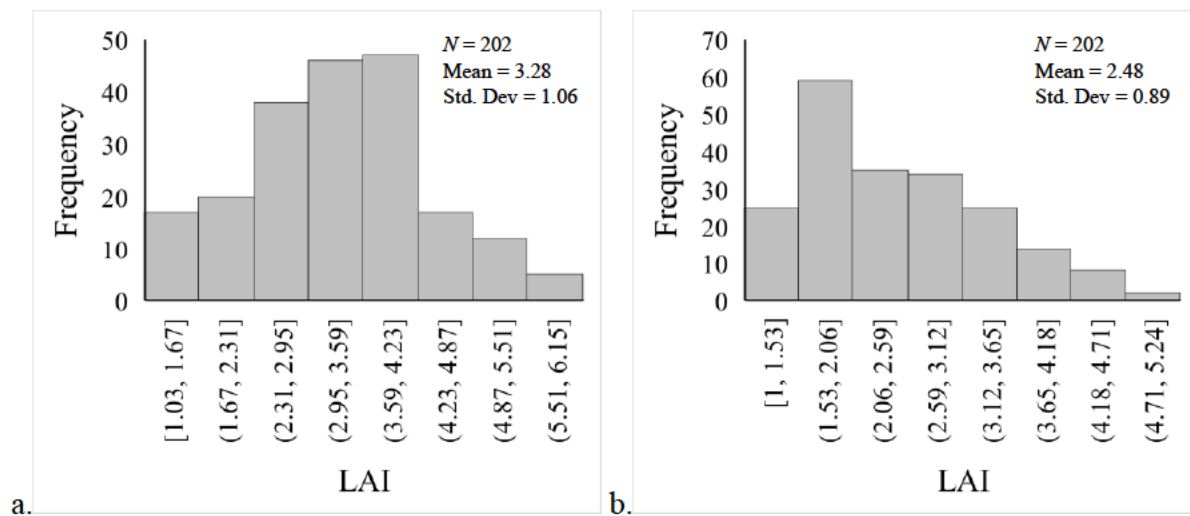


**Figure 3.3** Histogram showing LAIs over the study area in a) 2019 and b) 2022

In this study, scatterplots were used to assess the relationship between LAI measured by LiCor-2200 and LAI measured through destructive sampling. The results in Figure 3.4 show that LAIs measured by LiCor-2200 and LAI measured through destructive sampling are highly correlated with coefficients of determination of  $R^2=0.75$  and  $R^2=0.76$  for 2019 and 2020, respectively. Both the LiCor-2200 and destructive sampling techniques achieved comparable results.

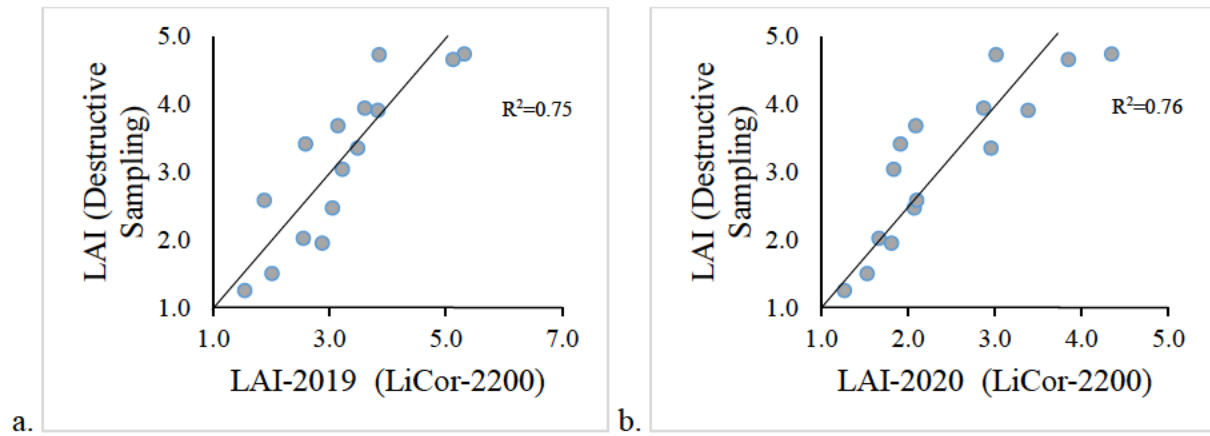
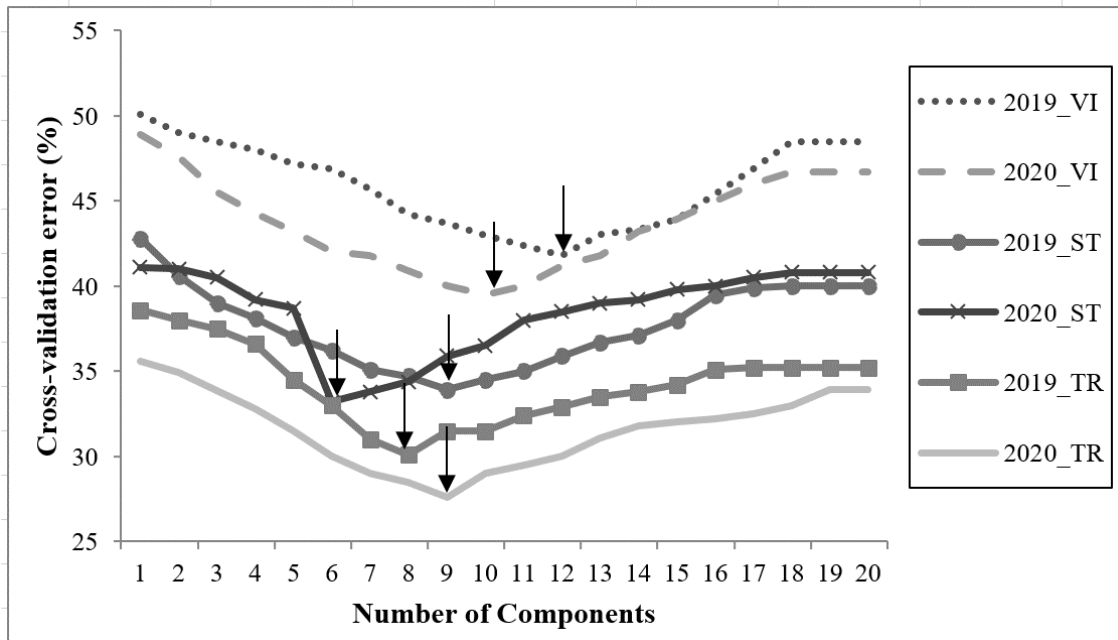


**Figure 3.4** Estimates of LAI derived from LiCor-2200 vs LAI derived from destructive sampling for a) 2019 and b) 2020

### 3.6.2 Optimising the PLS-R model

A 10-fold cross validation method was used to determine the number of components for optimal model development. Figure 3.5 shows that the number of optimal components for each model. According to Wolter et al., (2009), using fewer components is important for reducing model overfitting.



Key: VI – vegetation indices; ST – Single texture; TR – Texture ratios

**Figure 3.5** The number of components for each model

The black arrows indicate that the components with the lowest error for 2019 VI, 2020 VI, 2019 ST, 2020 ST, 2019 TR and 2020 TR were 12, 10, 9, 6, 8 and 9, respectively.

### 3.5.3 Using optimised PLS-R model to estimate LAI

Table 3.8 shows that integrating texture ratios into the model yielded higher estimation accuracy compared to the model that used vegetation indices and single texture bands only. The first model using a combination of vegetation indices had the lowest estimation accuracy, as it achieved an  $R^2$  of 0.59, RMSE= 1.38 in 2019 and  $R^2= 0.60$ , RMSE=1.40 in 2020 on the test dataset. The second model which had single texture bands achieved an  $R^2$  of 0.65, RMSE=1.35 in 2019 and  $R^2=0.67$ , RMSE=1.32 in 2020 based on the test dataset. The best performing model used texture ratios and it achieved an estimation accuracy of  $R^2=0.70$ , RMSE 1.21 in 2019 and  $R^2=0.72$ , M=RMSE=1.26 based on the test dataset. Since the PLS-R texture ratio model had the highest  $R^2$ , further analysis was done with this model.

**Table 3.8** Comparison between predictive PLS-R LAI models

PLS-R Model		2019		2020	
		R <sup>2</sup>	RMSE	R <sup>2</sup>	RMSE
Vegetation Indices	Test	0.59	1.38	0.60	1.40
	Train	0.60	1.34	0.61	1.36
Single texture bands	Test	0.65	1.35	0.67	1.32
	Train	0.63	1.33	0.66	1.34
Image texture ratios	Test	0.70	1.21	0.72	1.26
	Train	0.69	1.23	0.71	1.25

### 3.6.3 Frequency of significant variables selected by the PLS-R model

VIP selected 78 and 75 significant texture ratio parameters that yielded the highest overall classification accuracy for developing the PLS-R models for 2019 and 2020, respectively. However, we only illustrated the top ten selected ratios for developing the model in Table 3.9. Table 3.9 shows that mean, entropy and dissimilarity were the most frequently selected texture parameters for developing the 2019 and 2020 PLS-R texture ratio models. Results in Table 3.9 shows texture parameters that contain the majority of LAI information for 2019 and 2020. The texture ratios that contributed the most to the model were mean/entropy, mean/ second moment, mean/dissimilarity and mean correlation. These texture parameters were computed from the NIR-1, NIR-2, Red edge, red and green bands (Figure 3.6). This pattern was observed for both years. In terms of texture window size, both window sizes (3 x 3 and 5 x 5) performed well in the model, however the 3 x 3 window size frequency was higher than the 5 x 5 window size (Figure 3.6). The smaller window size, 3 x 3 in this case was better for detecting compartments that have high spectral variability.

**Table 3.9** Top 10 selected texture ratios selected by the PLS-R algorithm in 2019 and 2020

2019			2020		
Window Size	Band	Texture Ratio	Window Size	Band	Texture Ratio
3 × 3	NIR-1	Mean/Entropy	3 × 3	NIR-1	Mean/Entropy
3 × 3	NIR-2	Mean/Entropy	3 × 3	NIR-2	Mean/Entropy
3 × 3	NIR-2	Mean/Entropy	3 × 3	RED	Mean/Entropy
5 × 5	RED EDGE	Mean/Entropy	3 × 3	RED EDGE	Mean/ Homogeneity
5 × 5	RED	Mean/Second Moment	5 × 5	NIR-1	Mean/Second Moment
3 × 3	GREEN	Mean/Dissimilarity	3 × 3	RED	Mean/Dissimilarity
5 × 5	NIR-1	Mean/Second moment	5 × 5	GREEN	Mean/Homogeneity
3 × 3	RED EDGE	Mean/Correlation	3 × 3	NIR-1	Mean/Correlation
3 × 3	RED	Mean/Second moment	5 × 5	RED EDGE	Mean/Dissimilarity
5 × 5	RED	Mean/Second Moment	3 × 3	RED	Mean/Second Moment



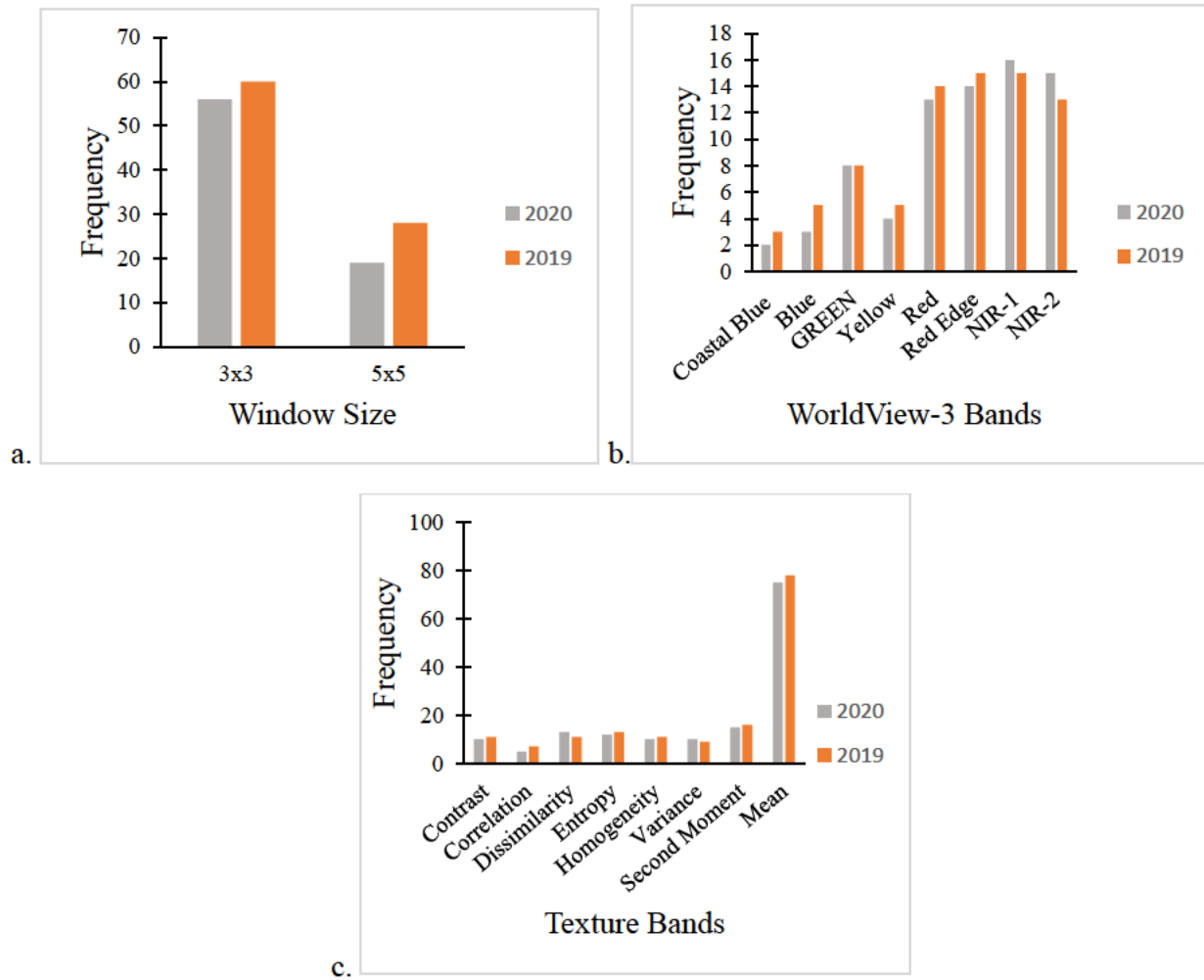


**Figure 3.6** Frequency of selected parameters: a) window size, b) WorldView-3 bands and c) Image texture parameters using the PLS-R algorithm

#### 3.6.4 Mapping the spatial distribution LAI using image texture ratios and PLS-R

Predictive maps displaying the distribution LAI was then created using the image texture ratio model for 2019 and 2020, as it yielded the highest accuracy. The predictive maps were developed using the R statistical package version 3.1.3. Figure 3.6 represents the spatial distribution of LAI over the dry and wet season.

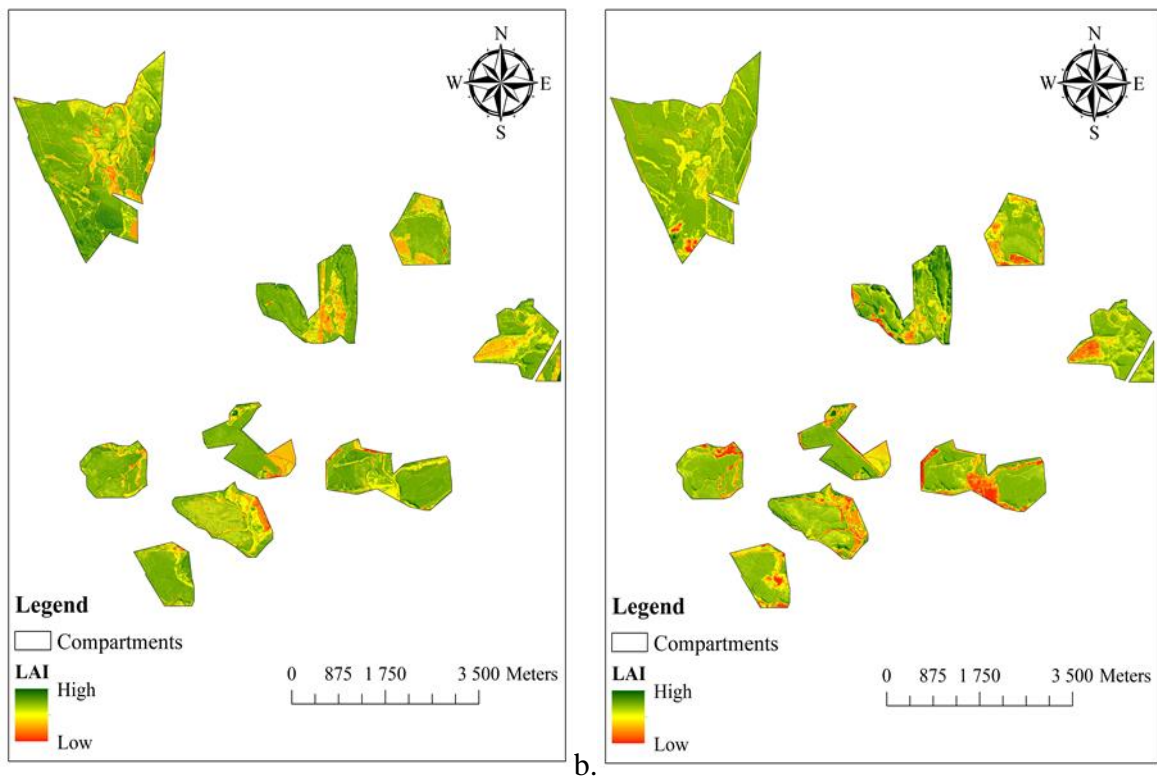


**Figure 3.7** LAI over the study area for a) 2019 and b) 2020 using image texture ratio

### 3.6.5 Relationship between LAI and Age

The LAI values recorded for compartments of the same age group from the same season are significantly different. For instance, the LAI value of F021 at canopy closure was 5.12 whereas the LAI value of A006 at canopy closure phase was 3.83 (Table 3.10). The difference in LAI values could be mainly attributed to the difference in stand density and site quality. The results also show that there are significant differences among phenological phases, compartments that are at canopy closure phase have the highest LAI compared to older compartment which are at the end of rotation, the LAI values start declining at mid rotation, and then older compartments at the end of rotation have the smallest LAI. It was observed from the results that younger compartments that are at canopy closure phase had the highest LAI.

**Table 3.10** Showing LAI values of compartments (compt) at different phenological phases

Compt no.	Phase	2019 LAI	2020 LAI	Destructive sampling LAI
E024	Canopy closure	5.31	4.35	4.74
F021	Canopy closure	5.12	3.85	4.66
A006	Canopy Closure	3.83	3.38	3.91
D016	Canopy closure	3.48	2.96	3.35
C030	Canopy Closure	3.85	3.01	4.73
D036	Mid rotation	3.60	2.87	3.94
D021	Mid rotation	3.05	2.07	2.47
D010A	Mid rotation	3.14	2.09	3.68
A001	Mid rotation	2.59	1.91	3.41
D001	Mid rotation	2.87	1.81	1.95
A005	End of rotation	3.22	1.83	3.04
F043	End of rotation	2.55	1.67	2.02
B001	End of rotation	1.88	2.10	2.58
B003	End of rotation	2.01	1.53	1.5
A011	End of rotation	1.54	1.27	1.25

In addition to the correlation analysis, scatterplot was used to illustrate the relationship between destructive sampling and age, 2019 wet season LAI and age, and lastly 2020 dry season and age. The results of this study show that there is a strong relationship between LAI collected through destructive sampling ( $R^2= 0.75$ ) (Figure 3.8). Younger compartments at canopy closure and mid rotation exhibited higher LAI compared to older compartments that were at the end of rotation. This could be attributed to younger compartments having wider fresh leaves and dense canopies, it was observed during the harvesting of the older compartments' leaves that they tended to have narrower and often dry or damaged leaves; hence low LAI.

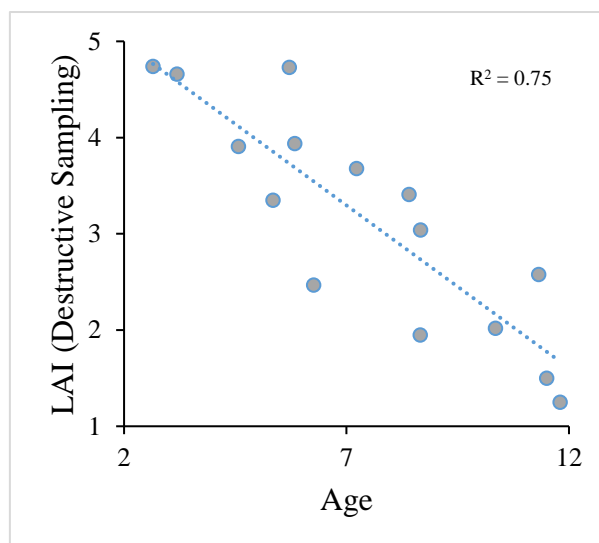


**Figure 3.8** Relationship between destructive sampling LAI and age

The results demonstrated that there is a strong relationship between LAI obtained through LiCor-2200 and age. These results also depict seasonal variations in LAI. The dry season had lower LAI values compared to the wet season. The correlation coefficient for the wet season 2019 LAI and age was the highest at  $R^2 = 0.91$  while the dry season achieved  $R^2 = 0.80$ . Figure 3.9 depicts the relationship between LiCor-2200 LAI and age.

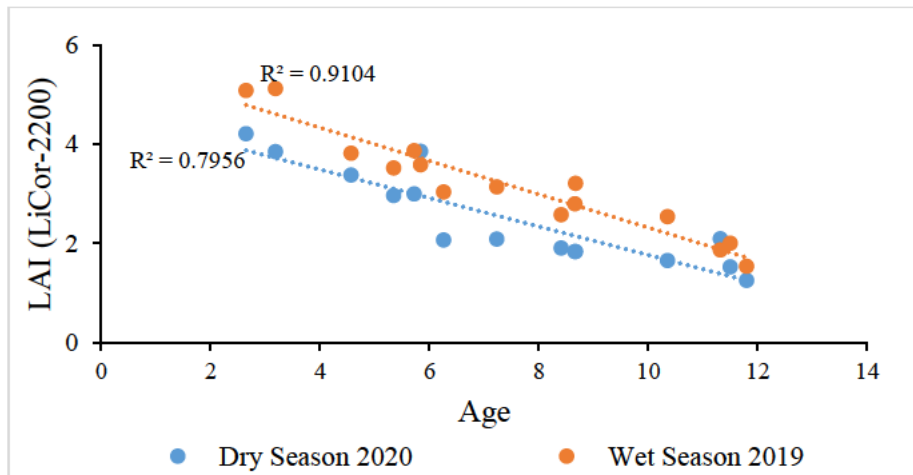


**Figure 3.9** Relationship between destructive sampling LAI and age

## 4. Discussion

The aim of the study to assess the utility of WorldView-3 vegetation indices and image texture for the estimation of LAI. The relationship between LAI and vegetation indices (VI) and texture with VIs was modelled using Partial Least Squares Regression (PLSR). The study tested the performance of three different image processing techniques to select the best performing model. The discussion will focus on 1. The relationship between LAI and image texture ratios and 2. The spatial distribution of LAI over the two growing seasons.

### 4.1 The relationship between LAI and image texture ratios

While all three techniques (vegetation indices, single texture bands and texture ratios) were successful in estimating the LAI for both seasons, the findings of this study demonstrate that texture ratios were capable of estimating LAI with higher accuracies. The Vegetation Indices (VI) technique produced the lowest accuracy (wet season:  $R^2=0.59$ , RMSE=1.38; dry season:  $R^2=0.60$ , RMSE=1.40), while single texture bands showed an improvement (wet season:  $R^2=0.65$ , RMSE=1.35; dry season:  $R^2=0.67$ , RMSE=1.32), the highest overall accuracy was, however, observed when texture ratios were incorporated into the model (wet season:  $R^2=0.70$ , RMSE=1.21) (dry season:  $R^2=0.72$ , RMSE=1.26).

The results of this study confirm the findings of previous studies that reported a significantly higher correlation between LAI and texture parameters. For example, Shamsoddini et al., (2013) assessed the potential of 11 GLCM texture measures and vegetation indices extracted from 8 WorldView-2 bands in mapping forest structural attributes. Their findings showed that incorporating texture parameters into the model improved the accuracy of mapping forest structural attributes. In a separate study, Gu et al., (2013) also assessed the ability of 4 IKONOS-2 texture band parameters and vegetation indices in estimating urban forest LAI and found that the performance of texture parameters was higher compared to vegetation indices. These findings demonstrate texture parameters contain additional valuable information about forest structural attributes such as LAI. This study's analysis also proves that texture parameters provide an alternate opportunity for improving the development of more accurate local LAI maps.

The significant improvement of LAI estimations in this study can be attributed to higher spatial and spectral resolution of WorldView-3 images. A number of studies have demonstrated the significance of spatial and spectral resolution in improving LAI estimations (Pu and Cheng,

2015, Lottering et al., 2018, Abdel-Rahman E.M et al., 2014). (Gebreslasie et al., 2008) tested the effects of spectral resolution in estimating forest structural attributes and concluded that using higher spatial resolution sensors to estimate forest structural attributes increases estimation accuracy by up to 19.7%.

One of the important steps in developing a model for estimating LAI is selecting an optimum number of bands or regions. This study found that NIR, Red edge, red, green bands are highly correlated to and strongly influence LAI. These results are consistent with the findings of Davhula (2016) and Feng et al., (2019). For instance, the NIR band generated the most influential GLCM statistical features for the estimation of LAI. NIR is sensitive to chlorophyll content and vegetation structure (Jordan, 1969). The Red edge band also contributed the most suitable GLCM variables. In addition, the mean and entropy texture features computed from NIR-1 made the highest contribution to model development. This indicates that the relevant information about vegetation attributes such as LAI is embedded in the red, green, red edge and NIR spectral regions. These findings are consistent with all the methods investigated; thus, they confirm that the red-edge band corresponds most to LAI. The direction of these findings was mainly influenced by vegetation structure as LAI is a component of vegetation structure, which influences the reflectance in the red, NIR and Red edge regions (Pu and Cheng, 2015). The use of single bands and vegetation indices for estimating LAI is common using hyperspectral data, but this study further demonstrated the improvement of LAI estimation using multispectral data. Furthermore, this study demonstrated that texture analysis can improve LAI estimations in regions of forest where spectral indices such as NDVI can saturate.

#### **4.2 Spatial distribution of LAI over the two seasons**

LAI distribution maps were created using the PLS-R model. The maps show the difference between 2019 (wet season) and 2020 (dry season). From the map it can be seen that the winter season had a lower LAI. The wet season has a relatively higher LAI. This is because LAI is affected by the supply of water, nutrients and temperature (White et al., 2010, Battaglia et al., 1998). In instances where there is enough supply of nutrients, water becomes the main determinant of LAI and tree growth (Benecke, 1980, Benson et al., 1992, Rubilar et al., 2013). Low water availability during the dry season hinders crop productivity. Furthermore, seasonal tree growth and defoliation of different functional types of leaf internal attributes lead to changes in the leaf lifespan and leaf area (Qiao et al., 2019). These findings align with those of Savoy and Mackay, (2015) and Ojeda et al., (2018). They also correspond with the findings

of (Zhu et al., 2016) where the lowest LAI was found in winter and the highest LAI was found in summer.

### 4.3 Conclusion

This study contributes to previous research studies on estimating LAI using high resolution, by incorporating two band texture ratios. It was able to develop a model that can accurately and efficiently estimate the LAI of *Eucalyptus dunnii* in the Midlands area, therefore addressing the needs of local forest managers. This study has shown that WorldView-3 imagery is capable of predicting LAI for two different seasons and can detect seasonal differences in LAI. Furthermore, this study revealed that:

- The texture ratio model produced higher LAI estimation accuracy when compared to vegetation indices and single image bands.
- The PLS-R model effectively mapped the spatial distribution of LAI over the two seasons.
- The predictive maps show that LAI was highest during 2019 (the wet season) and lowest during 2020 (the dry season).

Overall, this study was the first to utilize texture ratios to detect and map the spatial distribution of LAI using PLS-R over the wet and dry seasons. This study contributed to the body of literature and evidence that conclusively demonstrates the significance of using image texture ratios and PLS-R to effectively estimate LAI.

## 5. Synthesis

LAI is a very important parameter in plant ecophysiology and it can be used to directly quantify foliage and as a measure of the photosynthetic active area and thus the area subject to transpiration in the tree crown (Chen, 2013a; Wulder, Hall, Coops, & Franklin, 2004). Therefore, accurate estimation of LAI is crucial for optimal forestry management. Furthermore, understanding the spatial and temporal variation of LAI is particularly essential for silvicultural operations that are aimed at enhancing wood production, water yield and thus the overall stand productivity.

Using traditional methods of estimating LAI has been a serious challenge for large scale commercial forestry as these methods are time consuming, costly and impractical over large

forestry holdings. However, the advancements in remote sensing technology has offered a faster and effective method of estimating LAI with acceptable accuracies. This study reviewed methods of estimating LAI, found that there is an increasing pattern in the use of machine learning algorithms for the estimation of LAI. This is because of their advantage when it comes to handling big data sets. Moreover, the development of high spatial and spectral resolution sensors such as WorldView-3 has enabled scientists around the world to more effectively monitor vegetation attributes at higher accuracy (Kross et al., 2014).

One of the commonly used remote sensing methods of deriving LAI from spectral data is the empirical-based approach. In this approach regression models are used to study the relationship that exist between the target variable, for example, LAI and its spectral reflectance (Darvishzadeh et al., 2008a and 2012). The main objective of this study was to estimate LAI of *Eucalyptus dunnii* using high resolution WorldView-3 imagery in Midlands region of KwaZulu-Natal Province, South Africa. Our study utilised PLS-R to model the relationship between LAI and vegetation indices (VI), and texture with LAI. Among the three PLS-R models that were tested, the PLS-R texture ratio model had the highest  $R^2$  and lowest RMSE (wet season:  $R^2$  0.70, RMSE=1.21) (dry season:  $R^2$ =0.72, RMSE=1.26).

The use of vegetation indices did not yield the highest accuracy, this can be attributed to saturation of vegetation indices such as NDVI at LAI value above 3 (Zhou et al., 2014b). Generally, the best performing texture parameters were computed from the red, green, red edge and NIR1 and NIR2 bands. This indicates that the relevant information about vegetation attributes such as LAI is embedded in the red, green, red edge and NIR spectral regions. NIR and red edge bands are known to relate strongly with vegetation structure while red and green are known to relate to chlorophyll content. Integrating texture variable calculated from the best performing spectral bands led to increased LAI estimation accuracy.

### **5.1 Future research and recommendations**

This study demonstrated that two band texture ratios can estimate LAI with high accuracy, however for future research;

- Explore the ability of three or more band texture combinations for the estimation of LAI.
- Map and estimate LAI of various seasons and determine bands and vegetation that are consistently significant in LAI estimation.



- Explore robust machine learning algorithms for LAI estimation at local scales.

## 5.2 Conclusion

The focus of this study was to estimate the LAI of *Eucalyptus dunnii* using high resolution WorldView-3 and texture features. In this chapter, the aim and objectives highlighted in Chapter one (introduction) will be reviewed.

## 5.3 Review of Objectives

The aim of this study was to assess the utility of WorldView-3 vegetation indices and image textures for the estimation of LAI of *Eucalyptus dunnii*.

### 5.3.1 Specific objectives reviewed

- Review remote sensing methods of estimating LAI for forests and crops.

In order to meet this objective, published studies on using remote sensing to estimate LAI between 2010 and 2020 were reviewed. This study found that there were a total of 168 research publications focusing on estimations of LAI for forests, crops, and grasslands, published from 23 different journal publications. Among many remote sensing methods of estimating LAI, the most commonly used was empirical models. The results of this study also showed that there is an increasing trend in the use of machine learning algorithms. Several studies reported similar results as this study (Omer et al., 2016, Lin et al., 2019, Xu et al., 2020)

- Test the utility of vegetation indices in estimating LAI of *Eucalyptus dunnii* in the Midlands over two seasons using PLS-R.

The second objective was met by extracting 23 vegetation indices from WorldView-3 images, and these vegetation indices were used as inputs into the model. Although the vegetation indices (VI) model produced acceptable accuracies, it was not the best performing model. It achieved an estimation accuracy of  $R^2=0.59$ , RMSE=1.38 for 2019 (wet season) and  $R^2=0.60$ , RMSE=1.40 for 2020 (dry season). These findings coincide with those of Gu et al., (2013), Gebreslasie and van Aardt, (2011) and Li et al., (2019). It can therefore be concluded that vegetation indices alone do not yield the highest LAI estimation accuracy.

- Test the utility of texture ratios in estimating LAI of *Eucalyptus dunnii* in the Midlands over two seasons using PLS-R.

To meet the third objective, various texture measures were extracted from WorldView-3 imagery to create texture combinations. VIP analysis selected 78 and 75 significant texture

ratio parameters that yielded the highest overall classification accuracy for developing the PLS-R models for 2019 and 2020, respectively. The best performing model incorporated texture ratios and it achieved an estimation accuracy of  $R^2=0.70$ , RMSE 1.21 for 2019 (wet season) and  $R^2=0.72$ ,  $M=RMSE=1.26$  for 2020 (dry season). These results align with a number of published studies, such as those of Pu and Cheng, (2015), Ozdemira and Karnielib, (2011) and Gu et al., (2013). Therefore, it was concluded that texture measures can be used to estimate LAI of *dunnii* with high accuracy.

- Test the utility of single texture bands in estimating LAI of *Eucalyptus dunnii* in the Midlands using PLS-R.

The fourth objective was met by comparing the  $R^2$  and RMSE of the single texture band model against the vegetation index model and the image texture ratio model. The single texture band model yielded adequate accuracy for both seasons (wet season:  $R^2=0.65$ , RMSE=1.35) (dry season:  $R^2=0.67$ , RMSE=1.32), however; it was not the best model. The PLS-R model that yielded best results for both seasons was the one that integrated image texture ratios. The dominant texture ratios for both seasons were mean/entropy, mean/second moment, mean/dissimilarity and mean/correlation. These results are similar to those obtained by Hlatshwayo et al., (2019). Based on the results obtained in this current study, it was concluded that the best technique in estimating LAI is image texture measures. These conclusions confirm the hypothesis that combining texture algorithms improves the estimation of LAI.

- Determine the best technique in estimating LAI and map spatial distribution over the different seasons.

The fifth objective was met by using three methods; the first was collecting destructive sampling data and deriving LAI to be used as a reference, the second was collecting field LAI using the LiCor-2200 plant canopy analyser and the third was deriving vegetation indices and texture measures from WorldView-3 images. The relationship between LAI and vegetation indices (VI) and texture measures with VIs was modelled using Partial Least Square Regression (PLS-R). Then the best model was selected based on highest  $R^2$  and lowest RMSE.

### 5.3.2 Concluding Remarks

The aim of this study was to determine the best method for estimating the LAI of *Eucalyptus dunnii* in the Midlands area of KZN. By integrating texture ratios into the PLS-R model, the model estimation accuracy increased. This study showed that PLS-R texture measures model can be used to estimate the LAI of *Eucalyptus dunnii* in the Midlands with high accuracy. In

addition, the predictive maps showed that 2019 (wet season) had higher LAI when compared to 2020 (dry season). These conclusions are drawn based on the findings throughout this thesis and answer key research questions posed in Chapter one:

- What are the trends in the use of remote sensing methods to estimable LAI?

A total of 168 publications on estimating LAI using remote sensing were reviewed. The analysis revealed that there are few studies focusing on using texture measures to estimate LAI.

- Are vegetation indices the best method of estimating LAI of *Eucalyptus dunnii* in the Midlands area?

Vegetation indices were computed from WorldView-3 images and tested against single image texture and two texture band ratios using PLS-R. It was concluded that vegetation indices can estimate LAI with adequate accuracy. However, they are not the best method of estimating LAI. The vegetation indices PLS-R model achieved an estimation accuracy of  $R^2=0.59$ ,  $RMSE=1.38$  for 2019 (wet season) and  $R^2=0.60$ ,  $RMSE=1.40$  for 2020 (dry season).

- Are texture band ratios effective in estimating LAI of *Eucalyptus dunnii* in the Midlands area?

Texture ratios extracted from WorldView-3 imagery were input into a PLS-R model and successfully estimated LAI of *Eucalyptus dunnii* with highest accuracy for both seasons. The  $R^2$  of the best model was 0.70,  $RMSE$  1.21 for 2019 (wet season) and 0.72,  $M=RMSE=1.26$  for 2020 (dry season).

- Can single texture bands produce the best accuracy in estimating LAI of *Eucalyptus dunnii* in the Midlands area?

Single texture ratios were computed from best performing bands and input into a PLS-R model. The single texture band model yielded adequate accuracy for both seasons (wet season:  $R^2=0.65$ ,  $RMSE=1.35$ ) (dry season:  $R^2=0.67$ ,  $RMSE=1.32$ ), however; it was not the best model.

- What is the best model in estimating LAI of *Eucalyptus dunnii* in the Midlands area using PLS-R?

This study revealed that the texture band ratio model is the best model in estimating LAI of *Eucalyptus dunnii* in the Midlands area when compared to vegetation indices and single texture band models.

Overall, this study demonstrated that texture band ratios can estimate LAI of *Eucalyptus dunnii* in the Midlands area with acceptable accuracy.

## References

- Abdel-Rahman E.M., Mutanga, O., Odindi, J., Adam, E., Odindo, A. & Romel., I. 2014. A comparison of partial least squares (PLS) and sparse PLS regressions for predicting yield of Swiss chard grown under different irrigation water sources using hyperspectral data. *Computers and Electronics in Agriculture*, 106, pp.11-19.
- Ahmed, T., Tiaan, L. F., Zhang, Y. & Ting, K. C. 2011. A review of remote sensing methods for biomass feedstock production. *Biomass and Bioenergy*, 35, pp. 2455-2469.
- Arnó, J., Vallès, J. M., Llorens, J., Sanz, R., Masip, J., Palacín, J. & Rosell-Polo, J. R. 2012. Leaf area index estimation in vineyards using a ground-based LiDAR scanner. *Precision Agriculture*, 14, pp. 290-306.
- Bannari, A., Morin, D., Huette, A. R. & Bonn, F. 1995. A review of vegetation indices. *Remote Sensing of Environment*, 13, pp. 95-120.
- Banskota, A., Wynne, R. H., Thomas, V. A., Serbin, S. P., Kayastha, N., Gastellu-Etchegorry, J. P. & Townsend, P. A. 2013. Investigating the utility of wavelet transforms for inverting a 3-D radiative transfer model using hyperspectral data to retrieve forest LAI. *Remote Sensing of Environment*, 5, pp. 2639-2659.
- Baret, F. & Guyot, G. 1991. Potentials and limits of vegetation indices for LAI and APAR assessment. *Remote Sensing of Environment*, 35, pp. 161-173.
- Bastin, J. F., Barbier, N., Couteron, P., Adams, B., Shapiro, A., Bogaert, J. & De Canniere, C. 2014. Above ground biomass mapping of African forest mosaics using canopy texture analysis: Toward a regional approach. *Ecological Applications*, 24, pp.1984-2001.
- Battaglia, M., Cherry, M. L., Beadle, C. L., Sands, P. J. & Hingston, A. 1998. Prediction of Leaf Area Index in eucalyptus plantations: effects of water stress and temperature. *Tree Physiology*, 17, pp. 512-528.
- Beckschafer, P., Mundhenk, P., Kleinn, C., Ji, Y., Yu, D. & Harrison, R. 2013. Enhanced structural complexity Index: An improved index for describing forest structural complexity. *Open Journal of Forestry*, 3, pp. 23-29.
- Benecke, U. 1980. Photosynthesis and transpiration of *Pinus radiata* D. Don under natural conditions in a forest stand. *Oecologia*, 44, pp. 192-198.
- Benson, M. L., Myers, B. J. & Raison, R. J. 1992. Dynamics of stem growth of *Pinus radiata* as affected by water and nitrogen supply. *Forest Ecology and Management*, 52, pp. 1580-1595. 52
- Blinn, C. E., House, M. N., Wayne, R. H., Thomas, V. A., Thomas, F. R. & Sumnall, M. 2019. Landsat 8 Based Leaf Area Index Estimation in Loblolly Pine Plantations. *Forests*, 10, pp. 222-239.

- Campos-Taberner, M. G.-H., F.J., Camps-Valls, G., Grau Muedra, G., Nutini, F., Crema, A. & Boschetti, M. 2016. Multitemporal and multiresolution leaf area index retrieval for operational local rice crop monitoring. *Remote Sensing of the Environment*, 187, pp. 102-118.
- Chason, J. W., Baldocchi, D. D. & Huston, M. A. 1991. A comparison of direct and indirect methods for estimating forest canopy leaf area. *Agricultural and Forest Meteorology*, 57, pp. 107-128.
- Chen, J. M. 2013a. Remote sensing of leaf area index of vegetation covers. *Remote Sensing of Natural Resources*; pp. 375-398.
- Chen, J. M. 2013b. Spatial uncertainty analysis when mapping natural resources using remotely sensed data. In: G. WANG, & Q.WENG, (Eds), *Remote Sensing of Natural Resources*. 1st ed. Place: Milliton Park, Abingdon, United Kingdom. CRC Press: Taylor and Francis Group.
- Chin, W. W. 1998 The partial least squares approach to structural equation modeling. *Journal of Business Research.*, 295, pp. 295-336.
- Cui, Y., Zhao, K., Fan, W. & Xu, X. 2011. Retrieving crop fractional cover and LAI based on airborne Lidar data. *Journal of Remote Sensing Letters.*, 15, 1276-1288.
- Cutini, A., Matteucci, G. & Mugnozza, G. S. 1998. Estimation of leaf area index with the Li-Cor LAI- 2000 in deciduous forests. *Forest Ecology and Management*, 105, pp. 55-65.
- Daff. 2015. *A Profile of the South African Forestry Market Value Chain* [Online]. Available: [www.daff.gov.za](http://www.daff.gov.za). [Accessed: 01 October 2021].
- Darvishzadeh, R., Wang, T., Skidmore, A., Vrieling, A., O'connor, B., Gara, T. W., Ens, B. J. & Paganini, M. 2019a. Analysis of Sentinel-2 and RapidEye for Retrieval of Leaf Area Index in a Saltmarsh Using a Radiative Transfer Model. *Remote Sensing*, 11, pp. 671-682.
- Davhula, A. 2016. *Assessment Of Vegetation Productivity In The Umfolozi Catchment Using Leaf Area Index (LAI) Devived From SPOT 6 Image*. Unpublished Thesis (MSc). University of KwaZulu-Natal.
- Dube, T. & Mutanga, O. 2015. Investigating the robustness of the new Landsat-8 Operational Land Imager derived texture metrics in estimating plantation forest aboveground 53 biomass in resourceconstrained areas. *ISPRS Journal of Photogrammetry and Remote Sensing*, 108, pp. 12-32.
- Dube, T., Mutanga, O., Adam, E. & Ismail, R. 2014. Intra-and-inter species biomass prediction in a plantation forest: testing the utility of high spatial resolution spaceborne multispectral RapidEye sensor and advanced machine learning algorithms. *Sensors*, 14, pp. 15348-15370.
- Fang, H., Jiang, C., Li, W., Wei, S., Baret, F., Chen, J. M., Garcia-Haro, J., Liang, S., Liu, R. & Myneni, R. B. 2013. Characterization and intercomparison of global moderate resolution leaf area index (LAI) products: Analysis of climatologies and theoretical uncertainties. *Journal of Geophysical Research:Biogeosciences.*, 118, pp. 529-548.

- Fang, H., Zhang, Y., Wei, S., Li, W., Ye, Y., Sun, T. & Liu, W. 2019. Validation of MODIS and GEOV2 Leaf Area Index (LAI) products over croplands in Northern China. *IGARSS 2019-IEEE International Geoscience and Remote Sensing Symposium*. Yokohama, Japan:IEEE.
- Feng, W., Wu, Y., He, L., Ren, W., Wang, Y., Hou, G., Wang, Y., Liu, W. & Guo, T. 2019. An optimized non-linear vegetation index for estimating leaf area index in winter wheat *Precision Agriculture*, 20, pp. 1157-1176.
- Fu, Z., Wang, J., Song, J., Zhou, H., Pang, Y. & Chen, B. 2011. Estimation of forest canopy Leaf Area Index using MODIS, MISR and LiDAR observations. *Journal of Applied Remote Sensing*, 5, pp. 530-549.
- Furniss, D., Weiersbye, I., Tongway, D., Stark, R., Margalit, N., Nel, H., Grond, E. & Witkowski, E. T. 2009. Deriving Indices Of Landscape Function From Spectral Reflectances Of Grassland And Savanna Surfaces On Gold Mines In South Africa. *IEEE International Geoscience and Remote Sensing Symposium*, 9. Place: IEEE.
- Gamon, J. A. & Surfus, J. S. 1999. Assessing leaf pigment content and activity with a reflectometer. *New Phytologist*, 143, pp. 105-117.
- Gao, F., Anderson, M., Kustas, W. & Houborg, R. 2014. Retrieving Leaf Area Index From Landsat Using MODIS LAI Products and Field Measurements. *IEEE Geoscience and Remote Sensing Letters*, 11, pp. 773-777.
- Gastellu-Etchegorry, J. P., Martin, E. & Gascon, F. 2004. DART: a 3D model for simulating satellite images and studying surface radiation budget. *International Journal of Remote Sensing*, 25, pp.73-96.
- Gebreslasie, M. T., Ahmed, F. B. & Jan, V. A. 2008. Estimating plot-level forest structural attributes using high spectral resolution ASTER satellite data in even aged Eucalypts 54 plantations in southern KwaZulu-Natal, South Africa. *Southern Forests*, 70, pp. 227-236.
- Gebreslasie, M. T. A., F.B & Van Aardt, J. A. N. 2011. Extracting structural attributes from IKONOS imagery for Eucalyptus plantation forests in KwaZulu-Natal, South Africa, using image texture analysis and artificial neural networks. *International Journal of Remote Sensing*, 32, pp. 7677-7701.
- Ghebremicael, S. 2003. Estimating Leaf Area Index (LAI) of Black Wattle. Unpublished Thesis (MSc). University of KwaZulu-Natal. Pietermaritzburg.
- Gitelson, A. & Merzlyak, M. N. 1994. Quantitative Estimation of Chlorophyll-a Using Reflectance Spectra: Experiments with Autumn Chestnut and Maple Leaves. *Journal of Photochemistry and Photobiology*, 13, pp. 247-252.
- Gitelson, A. A. 2004. Wide dynamic range vegetation index for remote quantification of biophysical characteristics of vegetation. *Journal of Plant Physiology*, 161, pp.165-173.
- Gitelson, A. A., Kaufman, Y. J. & Merzlyak, M. N. 1996. Use of a green channel in remote sensing of global vegetation from EOS-MODIS. *Remote Sensing of Environment*, 58, pp. 289-298.

- Gitelson, A. A., Zur, Y., Chivkunova, O. B. & Merzlyak, M. N. 2002. Assessing carotenoid content in plant leaves with reflectance spectroscopy. *Photoscience and Photobiology Sciences*, 75, pp. 272-281.
- Gitelson, A. A. M., M.N. & Chivkunova, O. B. 2001. Optical properties and nondestructive estimation of anthocyanin content in plant leaves. *Photochemical and Photobiological Sciences*, 74, pp. 38-45.
- Glenn, E., Huete, A., Nagler, P. & Nelson, S. 2008. Relationship Between Remotely-sensed Vegetation Indices, Canopy Attributes and Plant Physiological Processes: What Vegetation Indices Can and Cannot Tell Us About the Landscape. *Sensors*, 8, pp.452-465.
- Gobron, N., Pinty, B., Verstraete, M. M. & Widlowski, J. L. 2000. Advanced vegetation indices optimized for up-coming sensors: Design, performance, and applications. *Geoscience and Remote Sensing*, 38, pp. 2489-2505.
- Gong, P., Pu, R. & Miller, J. R. 1995b. Coniferous forest leaf area index estimation along the Oregon Transect using Compact Airborne Spectrographic Imager data. *Photogrammetric Engineering and Remote Sensing*, 61, p. 10. 55
- Goswami, S., Gamon, J., Vargas, S. & Tweedie, C. 2015. Relationships of NDVI, Biomass and Leaf Area Index(LAI) for Six key plant species in Barrow, Alaska,. Available: PeerJ PrePrints 3 : e913v1 <https://doi.org/10.7287/peerj.preprints.913v1>. [Accessed: 16 December 2021].
- Groten, S. M. E. 1993. NDVI – crop monitoring and early yield assessment of Burkina Faso. *International Journal of Remote Sensing*, 14, pp. 1495-1515.
- Gu, Z., Ju, W., Li, L., Li, D., Liu, Y. & Fan, W. 2013. Using vegetation indices and texture measures to estimate vegetation fractional coverage (VFC) of planted and natural forests in Nanjing city, China. *Advances in Space Research*, 51, pp. 1186-1194.
- Guijun, Y., Zhao, C., Lui, Q., Haung, W. & Wang, J. 2011. Inversion of a Radiative Transfer Model for estimating forest LAI from multisource and multangular optical remote sensing data. *IEEE Transactions on Geoscience and Remote Sensing*, p. 49.
- Haboudane, D., Miller, J. R., Pattey, E., Zarco-Tejada, P. J. & Strachan, I. 2004. Hyperspectral vegetation indices and novel algorithms for predicting green LAI of crop canopies: modeling and validation in the context of precision agriculture. *Remote Sensing of Environment*, 90, pp. 337-352.
- Hadaś, E. & Estornell, J. 2016. Accuracy of tree geometric parameters depending on the LiDAR data density. *European Journal of Remote Sensing*, 49, pp. 73-92.
- Haenlein, M. & Kaplan, A. M. 2004. A beginner's guide to partial least squares analysis. *Understanding Statistics*, 3, pp. 283-297.
- Hansen, P. M. & Schjoerring, J. K. 2003. Reflectance measurement of canopy biomass and nitrogen status in wheat crops using normalized difference vegetation indices and partial least squares regression. . *Remote Sensing of Environment*, 86, pp. 542-553.



- Hlatshwayo, S. T., Mutanga, O., Lottering, R. T., Kiala, Z. & Ismail, R. 2019. Mapping forest aboveground biomass in the reforested Buffelsdraai landfill site using texture combinations computed from SPOT-6 pan-sharpened imagery. *International Journal of Applied Earth Observation and Geoinformation*, 74, pp. 65-77.
- Holmgren, P. & Thuresson, T. 1998. Satellite remote sensing for forestry planning: a review. *Scandinavian Journal of Forest Research*, 13, pp. 90-110.
- Huete, A. R., Didan, K., Miura, T., Rodriguez, E. P., Gao, X. & Ferreira, L. G. 2002. Overview of the radiometric and biophysical performance of the MODIS vegetation indices. *Remote Sensing of Environment* 83, pp. 195-213. 56
- Huete, A. R., Liu, H. Q., Batchily, K. & Van Leeuwen, W. 1997. A comparison of vegetation indices over a global set of TM images for EOS-MODIS. *Remote Sensing of Environment*, 59, pp. 440-451.
- Ilangakoon, N., Gorsevski, P. & Anita, S. 2015. Estimating Leaf Area Index by Bayesian Linear Regression Using Terrestrial LiDAR, LAI-2200 Plant Canopy Analyzer, and Landsat TM Spectral Indices. *Canadian Journal of Remote Sensing*, 41, pp. 315-333.
- Inoue, Y., Peñuelas, J., Miyata, A. & Mano, M. 2008. Normalized difference spectral indices for estimating photosynthetic efficiency and capacity at a canopy scale derived from hyperspectral and Carbon dioxide flux measurements in rice. *Remote Sensing of Environment*, 112, pp. 156-172.
- Jacquemound, S. & Baret, F. 2000. "PROSPECT: A model of leaf optical properties spectra". *Remote Sensing of Environment*, 32, pp. 75-91.
- Jensen, R. & Binford, M. 2004. Measurement and comparison of Leaf Area Index estimators derived from satellite remote sensing techniques. *International Journal of Remote Sensing*, 25, pp. 4251-4265.
- Jonckheere, I., Fleck, S., Nackaerts, K., Muys, B., Coppin, P., Weiss, M. & Baret, F. 2004. Review of methods for in situ leaf area index determination: Part I. Theories, sensors and hemispherical photography. *Agriculture For Meteorologists*. pp. 19-35.
- Jordan, C. F. 1969. Derivation of leaf area index from quality of light on the forest floor. *Ecology*, 50, pp. 663-666.
- Kanemasu, E., Niblett, C., Manges, H., Lenhert, D., & Newman, M. 1974. Wheat: its growth and disease severity as deduced from ERTS-1. *Remote Sensing of Environment*, 3, pp. 255-260.
- Kaufman, Y. J. & Tanre, D. 1996. Atmospherically resistant vegetation index (ARVI) for EOS-MODIS. *IEEE Transactions on Geosciences and Remote Sensing*, 30, pp. 261-270.
- Kayitakire, F., Hamel, C. & Defourny, P. 2006. Retrieving forest structure variables based on image texture analysis and IKONOS-2 imagery. *Remote Sensing Of Environment*, 102, Pp. 390-401.

- Kiala, Z., Odindi, J. & Mutanga, O. 2017. Potential of interval partial least square regression in estimating leaf area index. *South African Journal of Science*, 113, pp. 1-9.
- Korhonen, L., Packalen, P. & Rautiainen, M. 2017. Comparison of Sentinel-2 and Landsat 8 in the estimation of boreal forest canopy cover and leaf area index. *Remote Sensing of Environment*, 195, pp. 259-274. 57
- Kraus, T., Schmid, M., Dech, S. W. & Samimi, C. 2009. The potential of optical high resolution data for the assessment of leaf area index in East African rainforest ecosystems. *International Journal of Remote Sensing*, 30, pp. 5039-5059.
- Kross, A., McNairn, H., Lapen, D., Sunohara, M. & Champagne, C. 2014. Assessment of RapidEye Vegetation Indices for estimation of biomass in corn and soyabean crops. *International Journal Applied Earth Observation and Geoinformation.*, 34, pp. 235-248.
- Kumbula, S. T., Mafongoya, P., Peerbhay, K. Y. & Lottering, R. T. 2019. Using Sentinel-2 Multispectral Images to map the occurrence of the Cossid Moth (*Coryphodema tristis*) in Eucalyptus Nitens Plantations of Mpumalanga, South Africa. *Remote Sensing*, 11, pp. 11-23.
- Kuusk, A. 2001. A two-layer canopy reflectance model. *Journal of Quantitative Spectroscopy and Radiative Transfer*, 71, pp.1-9.
- Kuusk, A., Kuusk, J. & Lang, M. 2019. A statistical forest reflectance model. *Remote sensing*, 11, pp. 2749-2766.
- Lavender, A. 2017. Earth observation satellites in space in 2017. *Pixalytics* [Online]. [www.pixalytics.com](http://www.pixalytics.com) [Accessed: 06 June 2020].
- Le Maire, G., Marsden, C., Verhoef, W., Ponzoni, F. J., Seen, D. L., Bégué, A., Stape, J.-L. & Nouvellon, Y. 2011. Leaf area index estimation with MODIS reflectance time series and model inversion during full rotations of Eucalyptus plantations. *Remote Sensing of Environment*, 115, pp. 586-599.
- Li, S., Yuan, F., Karim, S., Zheng, H., Cheng, T., Liu, X., Tian, Y., Zhu, Y. & Cao, W. 2019. Combination of color indices and texture of AUV based digital imagery for rice LAI estimation. *Remote Sensing*, 11, pp. 1763-1773.
- Li, X. & Strahler, A. H. 1985. Geometric-optical modeling of a conifer forest canopy. *IEEE Transactions on Geosciences and Remote Sensing*, 23, pp. 705-721.
- Liang, L., Di, L., Zhang, L., Deng, M., Qin, Z., Zhao, S. & Lin, H. 2015. Estimation of crop LAI using hyperspectral vegetation indices and a hybrid inversion method. *Remote Sensing of Environment*, 165, pp. 123-134.
- Liang, S., Cheng, J., Jai, K., Jaing, B., Liu, Q., Xiao, Z., Yao, Y., Yuan, W., Zhang, X., Zhao, X. & Zhou, J. 2021. Global Land Surface Satellite Product Suite. *Bulletin of the American Meteorological Society*, 102, pp. 323-337. 58

- Lim, K., Treitz, P., Wulder, M., St-Onge, B. & Flood, M. 2003. LiDAR remote sensing of forest structure. *Progress in Physical Geography*, 27, pp. 88-106.
- Lin, J., Pan, Y., Lyu, H., Zhu, X., Li, X., Dong, B. & Li, H. 2019. Developing a two-step algorithm to estimate the leaf area index of forests with complex structures based on CHRIS/PROBA data. *Forest Ecology Management*, 441, pp. 57-70.
- Liu, K., Zhou, Q., Wu, W., Xia, T. & Tang, H. 2016. Estimating the crop leaf area index using hyperspectral remote sensing. *Journal of Integrative Agriculture*, 15, pp. 475-491.
- Liu, Y., Ju, W., Chen, J., Zhu, G., Xing, B., Zhu, J. & He, M. 2012. Spatial and temporal variations of forest LAI in China during 2000–2010. *Chinese Science Bulletin*, 57, pp. 2219-2229.
- Lottering, L., Mutanga, O. & Peerbhay, K. 2018. Detecting and mapping levels of *Gonipterus scutellatus*-induced vegetation defoliation and leaf area index using spatially optimized vegetation indices. *Journal of Applied Remote Sensing*, 13, pp. 277-292.
- Lu, B. & He, Y. 2019. Leaf Area Index Estimation in a Heterogeneous Grassland Using Optical, SAR, and DEM Data. *Canadian Journal of Remote Sensing*, 45, pp. 618-633.
- Luedeling, E., Hale, A., Zhang, M., Bentley, W. J. & Dharmasri, L. C. 2009. Remote sensing of spider mite damage in California peach orchards. *International Journal of Applied Earth Observation and Geoinformation*, 11, pp. 244-255.
- Luo, S., Chen, J. M., Wang, C., Gonsamo, A., Xi, X., Lin, Y., Qian, M., Peng, D., Nie, S. & Qin, H. 2018. Comparative performances of airborne LiDAR height and intensity data for leaf area index estimation. *IEEE Journal of Selected Topics in Applied Earth Observations and Remote Sensing*, 11, pp. 300-310.
- Maccioni, A., Agati, G. & Mazzinghi, P. 2001. New vegetation indices for remote measurement of chlorophylls based on leaf directional reflectance spectra. *Journal of Photochemistry Photobiology*, 61, pp. 52-61.
- Macedo, F. L., Sousa, A. M. O., Gonçalves, A. C., Marques Da Silva, J. R., Mesquita, P. A. & Rodrigues, R. A. F. 2018. Above-ground biomass estimation for *Quercus rotundifolia* using vegetation indices derived from high spatial resolution satellite images. *European Journal of Remote Sensing*, 51, pp. 932-944.
- Mahlein, A.-K., Oerke, E.-C., Steiner, U. & Dehne, H.-W. 2012. Recent advances in sensing plant diseases for precision crop protection. *European Journal of Plant Pathology*, 133, pp. 197-209.
- Materka, A. & Strzelecki, M. 1998. Texture Analysis Methods—a Review. COST B11 report. Brussels: Technical University of Lodz, Institute of Electronics.
- Mkhabela, M. S., Bullock, P., Raj, S., Wang, S. & Yang, Y. 2011. Crop yield forecasting on the Canadian Prairies using MODIS NDVI data. *Agricultural Forest Meteorology*, 151, pp. 385-393.

- Mthembu, S. 2001. Estimating Leaf Area Index (Lai) of Gum Tree. Unpublished Thesis (MSc). University of KwaZulu-Natal. Pietermaritzburg.
- Murray, H., Lucieer, A. & Williams, R. 2014. Texture-based classification of sub-Antarctic vegetation communities on Heard Island. *International Journal of Applied Earth Observation and Geoinformation*, 12, pp. 138-149.
- Nilson, T., Kuusk, A., Lang, M. & Lukk, T. 2003. Forest reflectance modelling: Theoretical aspects and applications. *Remote Sensing of the Environment*, 32, pp. 535-541.
- Ojeda, H., Rubilar, R., Montes, C., Cancino, J. & Espinosa, M. 2018. Leaf Area and growth of Chilean radiata pine plantations after thinning across a water stress gradient. *New Zealand journal of Forestry Science*, 48, pp. 1-11.
- Omer, G., Mutanga, O., Abdel-Rahman, E. & Adam, E. 2016. Empirical prediction of leaf area index (LAI) of engendered tree species in intact and fragmented forests ecosystems using WorldView-2 data and two robus machine learning algorithms. *Remote Sensing*, 8, pp. 324-351.
- Ozdemira, I. & Karnielib, A. 2011. Predicting forest structural parameters using the image texture derived from WorldView-2 multispectral imagery in a dryland forest, Israel. . *International Journal of Applied Earth Observation and Geoinformation* 13, pp. 701-710.
- Peduzzi, A., Wynne, R. H., Fox, T. R., Nelson, R. F. & Thomas, V. A. 2012. Comparative performances of airborne LiDAR height and intensity data for leaf area index estimation. *IEEE Journal of Selected Topics in Applied Earth Observation and Remote Sensing*, 11, pp. 300-310.
- Peerbhay, K., Y., Onesimo, M. & Ismail, R. 2013. "Investigating the capability of few strategically placed Worldview-2 multispectral bands to discriminate forest species in KwaZulu-Natal, South Africa. *IEEE Journal of Selected Topics in Applied Earth Observations and Remote Sensing*, 7, pp. 307-316.
- Peltzer, D. A., Bellingham, P. D., Dickie, I. & Philip, E. 2015. Commercial forests: Native advantage. *Science*, 349, pp. 1176-1176. 60
- Pope, G. & Treitz, P. 2013. Leaf Area Index (LAI) Estimation in Boreal Mixedwood Forest of Ontario, Canada Using Light Detection and Ranging (LiDAR) and WorldView-2 Imagery. *Remote Sensing*, 5, pp. 5040-5063.
- Potithec, S., Nagai, S., Nasahara, K. N., Muraoka, H. & Suzuki, R. 2013. Two separate periods of the LAI–VIs relationships using in situ measurements in a deciduous broadleaf forest. *Agricultural and Forest Meteorology*, 169, pp. 148-155.
- Potithec, S., Nasahara, N. K., Muraoka, H., Nagai, S. & Suzuki, R. 2010. What is the actual relationship between LAI and VI's in a deciduous broadleaf forest. *International Archives of the Photogrammetry. Remote Sensing and Spatial Information Science*, p. 38.
- Pu, R. & Cheng, J. 2015. Mapping forest leaf area index using reflectance and textural information derived from WorldView-2 imagery ina natural forest in Florida, US. *International Journal of Applied Earth Observation and Geoinformation*, 42, pp. 11-23.

- Qiao, K., Zhu, W., Xie, Z. & Li, P. 2019. Estimating the Seasonal Dynamics of the Leaf Area Index Using Piecewise LAI-VI Relationships Based on Phenophases *Remote Sensing*, 11, pp. 1-16.
- Qu, Y., Zhang, Y. & Wang, J. 2012. A dynamic Bayesian network data fusion algorithm for estimating leaf area index using time-series data from in situ measurement to remote sensing observations *International Journal of Remote Sensing*, 33, pp. 1106-1125.
- Quan, X., He, B., Yebra, M. & Yin, C. 2017. A radiative transfer model-based method for the estimation of grassland aboveground biomass *International Journal of Applied Earth Observation and Geoinformation*, pp. 1-10.
- Raymond Hunt Jr., E., Daughtry, C. S. T., H., J. U. & Long, D. S. 2011. Remote Sensing Leaf Chlorophyll Content Using a Visible Band Index. *Remote Sensing*, 103, pp. 1090-1099.
- Rivera, J. P., Verrelst, J., Leonenko, G. & Moreno, J. 2013. Multiple cost functions and regularization options for improved retrieval of leaf chlorophyll content and LAI through inversion of the PROSAIL model. *Remote Sensing*, 5, pp. 3280-3304.
- Roosjen, P. P., Brede, B., Suomalainen, J. M., Bartholomeus, H. M., Kooistra, L. & Clevers, J. G. 2018. Improved estimation of leaf area index and leaf chlorophyll content of a potato crop using multi-angle spectral data—potential of unmanned aerial vehicle imagery. *International Journal of Applied Earth Observation Geoinformation*, pp. 14-26. 61
- Rouse, J. W., Haas, R. H., Schell, J. A., Deering, D. W. & Harlan, C. J. 1974. Monitoring the Vernal Advancements and Retrogradation (Greenwave Effect) of Nature Vegetation. *NASA/GSFC Final Report*. Greenbelt, MD, USA: NASA.
- Rubilar, R., Albaugh, T., Allen, H. L., Alvarez, J., Fox, T. R. & Stape, J. 2013. Influences of silvicultural manipulations on above-and belowground biomass accumulations and leaf area in young *Pinus radiata* plantations, at three contrasting sites in Chile. *Forestry*, 86, pp. 27-38.
- Rubner, Y., Puzicha, J., Tomasi, C. & Buhmann, J. M. 2001. Empirical evaluation of dissimilarity measures for color and texture. *Computer Vision and Image Understanding*, 84, pp. 25-43.
- Sarker, L. R. & Nichol, J. E. 2011. Improved forest biomass estimates using ALOS AVNIR-2 texture indices. *Remote Sensing of Environment*, 115, pp. 968-977.
- Savoy, P. & Mackay, D. S. 2015. Modeling the seasonal dynamics of leaf area index based on environmental constraints to canopy development. *Agricultural and Forest Meteorology*, 200, pp. 46-56.
- Scharf, P. C. & Lory, J. A. 2002. Calibrating corn color from aerial photographs to predictsidedress nitrogen need contrib. from the Missouri Agric. Exp. Stn. J. Ser. No.13086. *Agronomy Journal*, 94, pp. 397-404.
- Shamsoddini, A., Trinder, J. C. & Turner, R. 2013. Pine plantation structure mapping using WorldView-2 multispectral image. *International Journal of Remote Sensing*, 34, pp. 3986-4007.

- Sibanda, M., Mutanga, O., Rouget, M. & Kumar, L. 2017. Estimating biomass of native grass grown under complex management treatments using WorldView-3 spectral derivatives. *Remote Sensing*, 9, pp. 55-76.
- Song, C. 2013. Optical remote sensing of forest leaf area index and biomass. *Progress in Physical Geography*, pp. 98-113.
- Sripada, R. P., Heiniger, R. W., White, J. & Weisz, R. 2006. Areal Color Infrared Photography for Determining Late-Season Nitrogen Requirements in Corn. *Agronomy Journal*, 97, pp. 322-335.
- Su, W., Huang, J., Liu, D. & Zhang, M. 2019. Retrieving corn canopy leaf area index from multitemporal landsat imagery and terrestrial LiDAR data. *Remote Sensing*, 11, pp. 572. 62
- Sun, Y., Qin, Q., Ren, H., Zhang, T. & Chen, S. 2020. Red-Edge band vegetation indices for Leaf Area Index estimation from Sentinel-2/MSI imagery. *IEEE Transactions on Geoscience and Remote Sensing*, 58, pp. 826-840.
- Team., R. D. C. 2015. *R: A Language and Environment for Statistical Computing*. [Online]. Available: <http://www.R-project.or> [Accessed: 06 November 2021].
- Thissen, U., Pepers, M., Ustun, B., Melssen, W. & Buydens, L. 2004. Comparing support vector machines to PLS for spectral regression applications. *Chemometrics and Intelligent Laboratory Systems*, 73, pp. 169-179.
- The EndNote Team, 2013. EndNote. EndNoteX9. Clarivate, Philadelphia, PA.
- Tian, Y. C., Yao, X., Yang, J., Cao, W. X., Hannaway, D. B. & Zhu, Y. 2011. Assessing newly developed and published vegetation indices for estimating rice leaf nitrogen concentration with ground- and space-based hyperspectral reflectance *Field Crops Research*, 120, pp. 299-310.
- Tillack, A., Clasen, A., Förster, M. & Kleinschmit, B. 2014. Estimation of Seasonal Leaf Area Index in an Alluvial Forest Using High Resolution Satellite-based Vegetation Indices. *Remote Sensing*, 141, pp. 52-63.
- Tucker, C. J. 1979. Red and photographic infrared linear combinations for monitoring vegetation. *Remote Sensing of Environment*, 8, pp. 127-150.
- Tuttle, E. M., Jensen, R. R., Formica, V. A. & Gonser, R. A. 2006. Using remote sensing image texture to study habitat use patterns: a case study using the polymorphic whitethroated sparrow (*Zonotrichia albicollis*). *Global Ecological Biogeography*, 15, pp. 349-357.
- Verger, A., Baret, F. & Camacho, F. 2011. Optimal modalities for radiative transfer-neural network estimation of canopy biophysical characteristics: Evaluation over an agricultural area with CHRIS/PROBA observations. *Remote Sensing of the Environment*, 115, pp. 415-426.
- Verrelst, J., Muñoz, J., Alonso, L., Delegido, J., Rivera, J. P., Camps-Valls, G. & Moreno, J. 2012. Machine learning regression algorithms for biophysical parameter retrieval: Opportunities for Sentinel-2 and-3. *Remote Sensing of the Environment*, 118, pp. 127-139.

- Viña, A., Gitelson, A. A., Nguy-Robertson, A. L. & Yi, P. 2015. Comparison of different vegetation indices for the remote assessment of green leaf area index of crops. *Remote Sensing of Environment*, p. 115. 63
- Vohland, M. & Jarmer, T. 2008. Estimating structural and biochemical parameters for grassland from spectroradiometer data by radiative transfer modelling (PROSPECT +SAIL). *Internal Journal of Remote Sensing*, 29, pp. 191-209.
- Wan, H. W., Wang, J. D., Liang, S. L. & Qin, J. 2009. [Estimating leaf area index by fusing MODIS and MISR data]. *Guang Pu Xue Yu Guang Pu Fen Xi*, 29, pp. 3106-11.
- Wang, R., Chen, J. M., Liu, Z. & Arain, A. 2017. Evaluation of seasonal variations of remotely sensed leaf area index over five evergreen coniferous forests. *ISPRS Journal of Photogrammetry and Remote Sensing*, pp. 187-201.
- Wang, T., Kang, F., Han, H., Cheng, X., Zhu, J. & Zhou, W. 2019. Estimation of leaf area index from high resolution ZY-3 satellite imagery in a catchment dominated by *Larix principis-rupprechtii*, northern China. *Journal of Forestry Resources*, 30, pp. 603-615.
- Wang, Y. & Fang, H. 2020. Estimation of LAI with the LiDAR Technology: A Review. *Remote Sensing*, 12, pp. 3457-3485.
- Waring, H. R., Coops, N. C. & Landsberg, J. J. 2010a. Improving predictions of forest growth using the 3-PGS model with observations. *Forest Ecology and Management*, 9, pp. 1722-1729.
- Waring, H. R., Coops, N. C. & Landsberg, J. J. 2010b. Improving predictions of forest growth using the 3-PGS model with observations. *Forest Ecology and Management*, 259, pp. 1722-1729.
- Waring, R. H. 1983. Estimating forest growth and efficiency in relation to canopy leaf area. *Advanced Ecological Resources*, 13, p. 26.
- Waser, T. L., Kuchler, M., Jutte, K. & Stampfer, T. 2014. Evaluating potential of WorldView-2 data to classify tree species and different levels of ash mortality. *Remote Sensing*, 6, pp. 4515-4545.
- Watson, D. 1947. Comparative Physiological Studies on the Growth of Field Crops. I. Variation in Net Assimilation Rate and Leaf Area between Species and Varieties and between Years. *Annals of Botany*, 11, p. 35.
- Wei, C., Huang, J., Mansaray, L. R., Li, Z., Liu, W. & Han, J. 2017. Estimation and Mapping of Winter Oilseed Rape LAI from High Spatial Resolution Satellite Data Based on a Hybrid Method. *Remote Sensing*, 9, p. 488.
- Weiss, M., Baret, F., Smith, G. J., Jonckheere, I. & Coppin, P. 2004. Review of methods for in situ leaf area index (LAI) determination. *Agricultural and Forest Meteorology*, 121, pp. 37-53. 64.

- White, D. A., Battaglia, M., Mendham, D. S., Crombie, D. S., Kinal, J. & Mcgrath, J. F. 2010. Observed and modelled leaf area index in Eucalyptus globulus plantations: tests of optimality and equilibrium hypotheses. *Tree Physiology*, 30, pp. 831-844.
- Wold, H. 1996. *Estimation of principal components and related models by iterative least squares*. Waltham, MA, USA: Academic Press.
- Wolter, P. T., Townsend, P. A. & Sturtevant, B. R. 2009. Estimation of Forest Structural Parameters Using 5 and 10 Meter SPOT-5 Satellite Data *Remote Sensing of Environment*, p. 113.
- Wulder, M. A., Hall, R. J., Coops, N. C. & Franklin, S. E. 2004. High Spatial Resolution Remotely Sensed data for ecosystem characterization. *Bioscience*, 54, p. 10.
- Xie, Q.-Y., Peng, D., Huang, W. & Casa, R. 2018. Vegetation Indices Combining the Red and Red-Edge Spectral Information for. *Applied Earth Observations and Remote Sensing*, ????.(vol, issue, pp.?)
- Xu, J., Quackenbush, L. J., Volk, T. A. & Im, J. 2020. Forest and Crop Leaf Area Index Estimation Using Remote Sensing: Research Trends and Future Directions. *Remote Sensing*, 12, pp. 1-32.
- Yan, G., Hu, R., Luo, J., Weiss, M., Jiang, H., Mu, X., Xie, D. & Zhang, W. 2019. Review of indirect optical measurements of leaf area index: Recent advances, challenges, and perspectives. *Agricultural and Forest Meteorology*, pp. 390-411.
- Yu, Y., Wang, J., Liu, G. & Cheng, F. 2019. Forest Leaf Area Index inversion based on Landsat OLI data in the Shangri-La city. *Journal of the Indian Society of Remote Sensing*, 47, pp. 967-976.
- Yuan, X., King, D. & Vlcek, J. 1991. Sugar maple decline assessment based on spectral and textural analysis of multispectral aerial videography. *Remote Sensing of Environment*, p. 37.
- Zhang, Z., He, G., Wang, X. & Jiang, H. 2011. Leaf area index estimation of bamboo forest in Fujian province based on IRS P6 LISS 3 imagery. *International Journal of Remote Sensing*, 32, pp. 5365-5379.
- Zhao, K., García, M., Liu, S., Guo, Q., Chen, G., Zhang, X., Zhou, Y. & Meng, X. 2015. Terrestrial lidar remote sensing of forests: Maximum likelihood estimates of canopy profile, leaf area index, and leaf angle distribution. *Agriculture for Meteorologists*, 209, pp. 100-113.
- Zheng, G. & Moskal, L. M. 2009. Retrieving leaf area index (LAI) using remote sensing: Theories, methods and sensors. *Sensors*, 9, pp. 2719-2745. 65
- Zhou, J., Zhao, Z., Zhao, J., Zhao, Q., Wang, F. & Wang, H. 2014a. A comparison of three methods for estimating the LAI of black locust (*Robinia pseudoacacia* L.) plantations on the Loess Plateau, China. *International Journal of Remote Sensing*, pp. 171-188.



Zhou, J.-J., Zhao, Z., Zhao, J., Zhao, Q., Wang, F. & Wang, H. 2014b. Comparison of three methods for estimating the LAI of black locust (*Robinia pseudoacacia* L.) plantations on the Loess Plateau, China. *International Journal of Remote Sensing*, 35, pp. 171-188.

Zhu, W., Xiang, W., Pan, Q., Zeng, Y., Ouyang, S., Lei, P., Deng, X., Fang, X. & Peng, C. 2016. Spatial and seasonal variations of leaf area index(LAI) in subtropical secondary forests related to floristic compositions and stand characters. *Biogeosciences*, 13, pp. 3819-3831.

Appendix 1 Destructive sampling LAI

Destructive sampling									LiCor-2200				
WF_wet	Sample_WF_wet	Sample_WF_Dry	Sample_Leaf_Area	Area/Tree	Leaf Area Tree	LAI	SLA	SLA	Ceptometer sample plot		Sample	LAI-2200-compartment LAI(Avg)	
kg	kg	kg	cm2	m2	m2	m2/m2	cm2/g	m2/kg	2019	2020	%	2019 LAI	2020 LAI
3.942	1.183	0.669	51213.88	6	17.07	2.844	76.55	7.655	1.65	1.45	0.3	1.54	1.26
4.471	1.341	0.604	32901.03	6	10.97	1.828	54.47	5.447	1.65	1.45	0.3	1.54	1.26
4.865	1.46	0.658	37141.29	6	12.38	2.063	56.45	5.645	1.65	1.45	0.3	1.54	1.26
7.091	2.127	1.057	67913.08	6	22.64	3.773	64.25	6.425	2.68	1.98	0.3	3.21	1.84
6.841	2.052	1.049	74333.49	6	24.78	4.13	70.86	7.086	2.68	1.98	0.3	3.21	1.84
7.113	2.134	1.077	70675.59	6	23.56	3.926	65.62	6.562	2.68	1.98	0.3	3.21	1.84
4.18	1.254	0.5	53893.62	7.5	17.96	2.395	107.79	10.779	4.95	4.91	0.3	5.08	4.21
7.743	2.323	0.979	105641.4	7.5	35.21	4.695	107.91	10.791	4.95	4.91	0.3	5.08	4.21
5.6	1.68	0.705	93014.53	7.5	31	4.134	131.94	13.194	4.95	4.91	0.3	5.08	4.21
4.002	1.2006	0.436	28102.38	6	9.37	1.561	64.46	6.446	2.61	1.93	0.3	2.8	1.84
3.424	1.027	0.486	34914.94	6	11.64	1.94	71.84	7.184	2.61	1.93	0.3	2.8	1.84
5.659	1.698	0.607	42521.39	6	14.17	2.362	70.05	7.005	2.61	1.93	0.3	2.8	1.84
6.219	1.866	1.029	80993.63	6	26.99	4.499	78.71	7.871	3.91	3.51	0.3	3.87	3
7.213	2.164	1.163	83916.25	6	27.97	4.662	72.15	7.215	3.91	3.51	0.3	3.87	3
9.165	2.749	1.206	90455.13	6	30.16	5.026	75	7.5	3.91	3.51	0.3	3.87	3
4.624	1.387	0.655	47479.06	6	15.83	2.638	72.49	7.249	2.49	3.77	0.3	3.82	3.38
3.893	1.168	0.517	43501.3	6	14.5	2.417	84.14	8.414	2.49	3.77	0.3	3.82	3.38
4.341	1.302	0.594	39414.29	6	13.14	2.19	66.35	6.635	2.49	3.77	0.3	3.82	3.38
5.967	1.79	0.893	69717.69	6	23.24	3.873	78.07	7.807	3.65	2.65	0.3	3.14	2.09
6.489	1.947	0.921	71975.41	6	23.99	3.998	78.15	7.815	3.65	2.65	0.3	3.14	2.09

5.389	1.617	0.814	57207.41	6	19.07	3.178	70.28	7.028	3.65	2.65	0.3	3.14	2.09
4.907	1.472	0.732	37458.71	6	12.49	2.081	51.17	5.117	1.32	1.83	0.3	2.01	1.53
3.885	1.166	0.595	33597.58	6	11.19	1.866	56.47	5.647	1.32	1.83	0.3	2.01	1.53
6.531	1.959	0.91	63995.9	6	21.34	3.556	70.33	7.033	1.32	1.83	0.3	2.01	1.53
3.543	1.063	0.525	38884.42	6	12.96	2.16	74.07	7.407	2.09	2.85	0.3	1.87	2.1
2.431	0.729	0.388	25401.58	6	8.47	1.412	65.47	6.547	2.09	2.85	0.3	1.87	2.1
2.315	0.695	0.395	21095.18	6	7.03	1.171	53.41	5.341	2.09	2.85	0.3	1.87	2.1
3.335	1.005	0.476	32965.07	6	10.94	1.823	69.25	6.925	2.05	2.19	0.3	2.58	1.91
2.127	0.638	0.32	19765.34	6	6.59	1.098	61.77	6.177	2.05	2.19	0.3	2.58	1.91
2.411	0.723	0.367	23372.88	6	7.79	1.299	63.69	6.369	2.05	2.19	0.3	2.58	1.91
4.29	1.286	0.621	44032.7	6	14.69	2.448	70.91	7.091	1.56	1.94	0.3	2.54	1.66
2.66	0.798	0.406	27037.86	6	9.01	1.502	66.6	6.66	1.56	1.94	0.3	2.54	1.66
3.778	1.133	0.57	37847.74	6	12.62	2.103	66.4	6.64	1.56	1.94	0.3	2.54	1.66
7.695	1.786	1.031	79206.98	6	34.13	5.688	76.83	7.683	5.09	4.64	0.23	5.12	3.85
5.954	1.829	0.941	75066.87	6	24.44	4.073	79.77	7.977	5.09	4.64	0.31	5.12	3.85
7.283	2.155	0.781	61562.93	6	20.81	3.468	78.83	7.883	5.09	4.64	0.3	5.12	3.85
5.755	1.726	0.704	56271.89	6	18.76	3.127	79.93	7.993	2.02	2.77	0.3	3.04	2.07
3.552	1.066	0.494	33276.46	6	11.09	1.848	67.36	6.736	2.02	2.77	0.3	3.04	2.07
4.446	1.334	0.564	43962.33	6	14.65	2.442	77.95	7.795	2.02	2.77	0.3	3.04	2.07
7.624	2.287	1.049	66126.96	6	22.04	3.674	63.04	6.304	3.71	3.72	0.3	3.59	3.86
7.962	2.387	1.081	83372.16	6	27.81	4.635	77.13	7.713	3.71	3.72	0.3	3.59	3.86
5.767	1.73	0.855	63061.96	6	21.02	3.504	73.76	7.376	3.71	3.72	0.3	3.59	3.86
3.122	0.937	0.456	52691.74	6	17.56	2.926	115.55	11.555	3.57	3.77	0.3	3.52	2.97
5.71	1.713	0.78	58536.69	6	19.51	3.252	75.05	7.505	3.57	3.77	0.3	3.52	2.97
6.401	1.92	0.855	69919.36	6	23.31	3.885	81.78	8.178	3.57	3.77	0.3	3.52	2.97

Appendix 2 List of countries and number of publications for each country

<b>Country Name</b>	<b>No. of Publications</b>	<b>Country Name</b>	<b>No. of Publications</b>	<b>Country Name</b>	<b>No. of Publications</b>
China	29	Botswana	1	Malawi	1
United States	21	Belgium	1	Mali	1
Brazil	16	Bolivia	1	Mozambique	1
Australia	11	Bulgaria	1	Niger	1
Canada	11	Burundi	1	Peru	1
Russia	10	Cambodia	1	Poland	1
South Africa	8	Chad	1	Philippines	1
Algeria	6	Congo	1	Saudi Arabia	1
Egypt	6	Cameroon	1	Senegal	1
Spain	5	Colombia	1	Sierra Leone	1
United Kingdom	5	Central African Republic	1	Sudan	1
India	4	Ethiopia	1	Sweden	1
New Zealand	4	France	1	United Arab Emirates	1
Finland	3	Ghana	1	Thailand	1
Germany	3	Greece	1	Turkey	1
Japan	3	Guinea	1	Tanzania,	1
Argentina	2	Hungary	1	Uganda	1
Zaire	2	Indonesia	1	Ukraine	1
Italy	2	Ivory Coast	1	Burkina Faso	1
Kenya	2	North Korea	1	Venezuela	1
Mexico	2	South Korea	1	Vietnam	1
Nigeria	2	Kazakhstan	1	Namibia	1
Netherlands	2	Liberia	1	Zambia	1
Angola	1	Libya	1	Zimbabwe	1
Austria	1	Lesotho	1		

Appendix 3 Models and sensors used for forest, crop and grassland studies and the level of accuracy achieved by each model

		Forest			Crop			Grassland			
Model	Sensors	N	R	RMS E	N	R	RMS E	N	R	RMS E	Algorithms
Empirical Models	VIs based	27	0.14-0.97	0.05-2.41	22	0.59-0.82	0.52-1.53	25	0.58-0.83	0.20-1.71	Wide range of VIs
	Reflectance based	15	0.58-0.97	0.10-1.08	9	0.45-0.95	0.03-1.82	10	0.36-0.95	0.02-1.83	Regressions
	Derived metrics	19	0.57-0.98	0.02-1.47	3	0.35-0.95	0.01-1.95	2	0.45-0.98	0.16-0.45	Regressions
	Machine Learning	8	0.84-0.95	0.43-1.95	13	0.58-0.97	0.34-1.94	9	0.44-0.97	0.14-1.66	ML Algorithms
Physical Models	PROSAIL	2	0.81-0.95	0.41-0.48	8	0.83-0.96	0.13-1.45	4	0.38-0.98	0.13-1.48	
	DART	2	0.75-0.87	0.46-0.52	0			0			Look up tables(LUT)
	PROSPECT+DART	1	0.77		0			0			Iterative optimization, LUTs
	4-Scale bidirectional reflectance distribution (BRD)	2	0.80-0.86	0.78-1.4	1	0.85	1.3	0			
	Other models	5	0.71-0.95	0.71-0.96	3	0.83-0.99	0.31-0.92	2	0.87-0.95	0.83-0.95	LUTs, dynamic model, etc.

Hybrid Models	PROSAIL	5	0.63-0.92	0.26-1.12	9	0.58-0.96	0.3-1,16	5	0.67-0.98	0.27-1.13	
	PARAS	2	0.83-0.93	0.71-0.85	0			0			Regression and ML algorithms
	4-Scale BRD	2	0.43-0.68	0.31-1.08	1	0.86	0.43	0			
	Other models	5	0.21-0.99	0.20-1.86	1	0.89	0.5	1	0.78	0.64	
Other models		6	0.41-.096	0.01-0.92	3	0.43-0.97	0.42-0.98	1	0.67-.099	0.01-1.94	Regional phenology model, path length distribution model, etc.